Graduate Theses and Dissertations

8-2017

Dental Microwear Textures of Paranthropus robustus from Kromdraai, Drimolen, and an Enlarged Sample from Swartkrans: Ecological and Intraspecific Variation

Alexandria Sachiko Peterson
University of Arkansas, Fayetteville

Follow this and additional works at: https://scholarworks.uark.edu/etd

Part of the Biological and Physical Anthropology Commons, and the Paleontology Commons

Dental Microwear Textures of *Paranthropus robustus* from Kromdraai, Drimolen, and an
Enlarged Sample from Swartkrans: Ecological and Intraspecific Variation

A thesis submitted in partial fulfillment
of the requirement for the degree of
Master of Arts in Anthropology

by

Alexandria S. Peterson
Loyola University Chicago
Bachelor of Science in Anthropology, 2014
Loyola University Chicago
Bachelor of Arts in Classical Civilizations, 2014

August 2017
University for Arkansas

This thesis has been approved for recommendation to the Graduate Council.

_____
Peter Ungar, PhD
Thesis Director

_____   _____
J. Michael Plavcan, PhD   Lucas Delezene, PhD
Committee Member   Committee Member

_____
Frederick Grine, PhD
Ex-Officio Committee Member

Abstract

The original microwear texture baseline for South African hominins was done by Scott et al. (2005) and concluded that *Paranthropus robustus* exhibited higher complexity values (*Asfc*) that are seen in occasional hard object feeders. *Australopithecus africanus* has higher anisotropy values (*epLsar*) consistent with consuming tough objects. This study expands upon this baseline by increasing the sample size from $n = 9$ for *P. robustus* and $n = 10$ for *Au. africanus* to $n = 66$ and $n = 44$, respectively. Additionally, this study incorporates multiple different sites and deposits. The *P. robustus* sample includes Drimolen, Kromdraai, and an expanded sample from Swartkrans, incorporating samples from Member 1 Hanging Remnant, Member 1 Lower Bank, Member 2, and Member 3. The *Au. africanus* sample expands the Sterkfontein sample and also incorporates Makapansgat.

White-light confocal microscopy in conjunction with scale-sensitive fractal analysis quantifies microwear texture variables. In addition, ISO parameters are also incorporated to further elaborate on specific attributes of texture patterns. ANOVA and MANOVA tests assess differences among central tendencies between taxa as well as among deposits. Pairwise tests assess differences in dispersion among *P. robustus* bearing deposits. Between taxa, the same complexity and anisotropy patterns seen in the previous study are also seen in this study. Among the *P. robustus* bearing deposits, there were no significant differences among central tendencies, but there were differences in dispersion. This suggests that while there is variation in textures among *P. robustus* samples, these differences are not outside the overall range seen for the species.

Acknowledgements

This project has involved a lot of people, and there are even more who have supported me throughout the entire process.

First and foremost, I am so appreciative to Dr. Peter Ungar for being the best of advisors. I've struggled a lot finishing this thesis, and he has been a constant source of inspiration and support. Thank you for providing me with perspective and guidance every time I came to your office in a panic, and for pushing me to keep moving forward and constantly improve my work. I look forward to continuing to work with you as an ENDY PhD student!

I'd like to thank my committee members. Thank you Dr. Luke Delezene and Dr. Mike Plavcan for your advice throughout the last two years and your insightful questions during my defense. I have learned a lot from taking classes with both of you and I greatly value your advice. Thank you also to Dr. Fred Grine for being an ex officio member of my committee and for your significant guidance on this project. Your expertise on *Paranthropus* and South African sites has been invaluable.

A special thank you to Dr. Mark Teaford. Your keen eye to microwear details has also been extremely helpful, and I've taken much of your feedback to heart. Moving forward, I will definitely have a sharper eye on removing junk from the surface of my scans!

Thank you to my family for their constant support and encouragement. And thank you for understanding when I couldn't come home for holidays because I was working in the lab. Thank you also to my graduate student cohort and my close friends from back home. You all were ready with an encouraging word and good advice on how to handle situations. Special

thanks as well to Sarah Livengood for keeping an eye on me and providing insight when I was a mess.

Finally, I am especially grateful to my academic sisters, Elicia Abella and Jenny Burgman. You both took me under your wing, are great mentors to me, and have become great friends. Thank you Elicia for all your help with data processing for this project. You've saved my bacon multiple times, and you always have my back. Thank you Jenny for your constant advice, both academic and health-wise, and all the times we made dinner and watched comedies. I am infinitely lucky to have a cohort who are not only great colleagues, but have truly become my academic family.

Dedication

This thesis is dedicated to my partner, Daniel Taylor. You've been there for all of my highs and lows. Thank you for you for believing in me when I wouldn't believe in myself. And I will always remember being in Chicago with you and working on this thesis. Thank you for all the coffee and sweets you got me while working, and for reading and editing all my terrible first drafts. This is for you.

Table of Contents

List of Tables

List of Figures

Introduction

Reconstructing the diet of an extinct animal is imperative to understanding its behavior, environmental context, and evolutionary history. Concerning early hominins, the genus *Paranthropus* is an evolutionary oddball, exhibiting a hyper-robust masticatory complex that presents an interesting conundrum between morphology and diet. Both the eastern African variant, *Paranthropus boisei*, and the South African variant, *Paranthropus robustus,* share large, thick facial and mandibular features in addition to exhibiting large, flat postcanine teeth with thick enamel (Rak 1983; Olejniczak et al. 2008). These adaptations are traditionally associated with hard object feeding, as robust cranial and facial bones along with thick enamel are seen in primates that eat hard foods as primary parts of their diet or as fallback foods (Rak 1983; Lambert et al. 2004; Wood and Strait 2004; Strait et al. 2008; Lambert 2009; Ungar and Daegling 2013). Jolly (1970) put forth the Seed-Eating hypothesis, where the upright posture used during seed eating drives selection for bipedalism. Additionally, wide, flat postcanine teeth with thick enamel provide a larger, more resilient surface area to crack harder outer casings and small hard objects while also still maintaining the ability to process other softer foods (Rak 1983; Kay 1985; Strait et al. 2004; Altmann 2009; Rabenold and Pearson 2011). Finite-element analysis of the face of *Au. africanus* sees stresses being higher in critical points of the face during heavy loading of the posterior teeth, which is also seen in a model of *Macaca fasicularis.* These sections of the face are more robust both in *Au. africanus* as well as both species of *Paranthropus* (Rak 1983; Strait et al. 2008; Strait et al. 2012). These assessments of the morphology of *Paranthropus* lead to the conclusion that the genus must be engaging in chewing

behaviors that require massive amounts of force to process hard objects. This hypothesis even lends itself to the nickname for *P. boisei,* the "Nutcracker Man."

With the incorporation of non-adaptive methods of dietary reconstruction, such as dental microwear and stable isotope analysis, dietary reconstruction becomes more complicated and is seemingly in conflict with conclusions drawn from functional morphology. Stable carbon isotopes in tooth enamel demonstrate that *Au. africanus,* and *P. robustus* share similar mixed C_3/ C_4 dietary signals while *P. boisei* has an almost exclusively C_4 dietary signal (Sponheimer et al. 2006; Cerling et al. 2011; Ungar and Sponheimer 2011). Microwear textures also reflect dietary behaviors by examining the record of features left on the enamel surface of the tooth that are indicative of crushing harder objects (pitting) or shearing tougher materials (striations) (Scott et al. 2006). Among the South African species, Grine (1981) found that the molars of *Au. africanus* have higher cusps with more scratches and more polishing, while *P. robustus* has lower, rounded cusps and more pitting (Ungar 2007). Building upon this, Scott et al. (2005) report microwear texture signatures for these South African hominins, suggesting a separation between *Au. africanus,* which has more variable anisotropic scratches, and *P. robustus*, which has more complex pitting. While there is overlap in textures, this suggests that *Au. africanus* had a tougher diet on average, and that *P. robustus* had more hard objects in its diet. Particularly, the pattern of pitting for *P. robustus* suggests that hard objects were not consumed as a staple food, but only occasionally throughout the year. Additionally, carbon isotope data and microwear data for *P. boisei* reflect a diet almost exclusively comprised of C_4 resources, possibly grasses or sedges, and there are even suggestions of termite foraging for both variants of *Paranthropus* (Sponheimer et al. 2005; Cerling et al. 2011).

These dietary reconstructions come into conflict with conclusions drawn from functional morphology and creates an interesting conundrum. These hominins are seemingly adapted for hard object feeding, but the non-adaptive "foodprints" (Ungar, 2017) are not consistent with a diet dominated by such items. There are three possible explanations for the evolution of these robust morphologies: 1) hard object food primary adaptation; 2) hard object food fallback adaptation; and 3) sub-optimal adaptation for grinding tough foods.

Hard-object preference

The traditional interpretation of the *Paranthropus* form-function relationship involves the incorporation of hard objects as a preferred, regularly consumed food. According to this model, morphological adaptations such as large masticatory muscles, robust facial buttressing, and large, flat postcanine teeth with thick enamel caps are selected for because of habitual hard object feeding (Rak 1983; Lucas et al. 2008). An early overview of hominin dentition done by Robinson (1954b) concluded that the teeth of *Paranthripus* was best suited for crushing and grinding vegetation, as opposed to the more omnivorous diet of *Australopithecus*. An analysis of enamel thickness also points to thicker enamel and decussaation of enamel prisms being an adaptive response to resist cracks, especially when consuming hard objects (Lucas et al. 2008). Further, Wood and Constantino (2007) detail fifty years of research on the eastern African variant of the genus, *P. boisei*. The hyper-thick enamel, megadont and bunodont molars, and large muscle attachments of *P. boisei* point to the mastication of either very hard or very tough objects, and its small anterior teeth suggest *P. boisei* is eating foods that do not require incisal preparation (Hylander 1975). Because of the close evolutionary relationship posited between *P. boisei* and *P.*

robustus, both species were presumed to be engaged in hard object feeding based on morphology

and tooth enamel (Kay 1985; Wood and Constantino 2007; Lucas et al. 2008). Studies using

finite element analysis also point to hard object feeding being the selective pressure behind the

facial robusticity seen in hard object feeding primates and purported hard object feeding

hominins (Strait et al. 2009). However, these studies do not explain why isotopic and microwear

signatures are so disparate with functional morphology. Proponents of this model dismiss the

microwear evidence and postulate that the C4 isotopic signature is reflecting a C4 hard object

food for *P. boisei* (Strait et al. 2013). Additionally, Constantino et al. (2010) argue that enamel

chipping more closely reflects the bite forces needed for hard object feeding that microwear and

isotopic analysis may miss. In contrast, Daegling et al. (2013) suggest that morphological

adaptation frame what an organism is capable of eating while microwear and isotopes provide

snapshots of individual behavior in a small window of time.

Fallback food adaptation

Another explanation for *Paranthropus* cranio-dental functional morphology involves an

adaptation for fallback foods. Fallback foods are critical resources used only preferentially when

favored resources are unavailable, especially during times of resource stress. These items can

also provide a selective pressure on morphology (Altmann 2009; Constantino and Wright 2009;

Constantino et al. 2009). Liem's Paradox explains how an animal is adapted for processing

critical food resources that are only utilized during times of resource stresses. Their morphology

is then adapted for effectively finding and processing these critical resources that are only eaten

when the preferred staple food of the animal is unavailable, similar to how gorillas have sharp

shearing crests and large chewing muscles that are effective for processing fibrous vegetation, but will prefer to eat fruit first when it is available (Remis, 2002; Harrison and Marshall, 2011). This is consistent with both the adaptive evidence and the microwear and isotope signatures for eurytopy in *P. robustus* – but not the foodprint evidence for stenotopy in *P. boisei* (Wood and Strait, 2004). However, character displacement may account for some of the differences seen in sympatric primate species, leading to diverging behaviors (Hansen et al. 2000; Nun and Barton 2001). Chimpanzees and gorillas have considerable overlap in their diets, but have dietary adaptations that diverge and result in both different morphologies and behaviors, which includes what fallback foods are utilized during times of resource stress (Remis 2002; Harrison and Marshall, 2011)

Suboptimal adaptation

Finally, the last explanation proposes that *Paranthropus,* in particular *P. boisei*, has suboptimal occlusal morphology – lacking sharp shearing crests but rather, developing a large, flat occlusal surface for processing tough, fibrous foods, and requiring significant development of the jaw and chewing muscles to make up for the lack of occlusal relief to shear items (Daegling et al 2011, 2013, Ungar and Hlusko 2016; Daegling and Grine 2017). This last hypothesis is consistent with both the adaptive evidence and the microwear and isotope signatures in *P. boisei* – but not the foodprint evidence in *P. robustus*.

Evaluation of these hypotheses are predicated on the accurate and complete characterization of diets of these hominins by both adaptive and non-adaptive lines of evidence. And while there are hundreds of individual fossil specimens known for some of these taxa,

including South African species of hominins such as *Au. africanus* and *P. robustus*, sample sizes have been limited in some analyses. Dental microwear presents a case in point. Texture analysis is an analytical method that utilizes microscopic wear evidence to provide data on both the material properties of the foods consumed as well as the angle of attack of chewing behaviors. Analyses of primate diets are able to distinguish between hard and tough food properties in the diet (Scott et al. 2005; Scott et al. 2006; Scott et al. 2012). Microwear texture analysis is also utilized in a wide array of mammalian and fossil studies for both dietary and environmental assessment.

Nevertheless, analyses of dental microwear textures on *P. robustus* from Swartkrans and Kromdraai and *Au. africanus* from Sterkfontein involved a smaller sample of fossils in comparison with a known baseline of primate microwear textures, verified with dietary observations (Scott et al. 2005; Scott et al. 2012). However, larger samples of these early hominins are known from these three sites, with more recent excavations also incorporating the sites of Drimolen (*P. robustus*) and Makapansgat (*Au. africanus*). The principal goal of this thesis are to expand upon the previous hominin microwear texture analysis by including all available specimens of *P. robustus* (Scott et al. 2005). This includes a broad sample of molars spanning Kromdraai, Drimolen, and all the hominin bearing deposits at Swartkrans This effectively increases the sample size of *P. robustus* microwear from $n = 9$ from Swartkrans Member 1 Hanging Remnant and Kromdraai, to $n = 68$ from three sites, including more deposits from Swartkrans: Member 1 Lower Bank, Member 2 and Member 3. With a larger sample, the question becomes whether the pattern of textures evinced by *P. robustus*, as described by Scott et al., (2005) is preserved, and can still be distinguished from that of *Au. africanus*.

The larger sample also allows consideration of variation within *P. robustus* but between deposits from which samples were recovered. The previous sample of $n = 9$ specimens, $n = 8$ specimens from Swartkrans Member 1 Hanging Remnant and $n = 1$ specimen from Member 3 of Kromadraai. Expanding the sample size for *P. robustus* and incorporating more individuals from multiple sites creates a more robust sample size in order to assess variation in microwear, and by extension, diet between the samples for the species. This will allow us to better assess hypotheses concerning whether the microwear textures of *P. robustus* are indicative of a form-function relationship consistent with a preferred food adaptation for hard objects, a fallback adaptation for hard objects, or a suboptimal adaptation for tough, abrasive foods. This will help to assess whether food preferences varied between samples and environments represented by the various sites and deposits in which *P. robustus* has been found.

The remainder of this introduction will present an historical background to *P. robustus*, a description of the sites and their habitat reconstructions, and a brief review of microwear texture analysis to put the current study in context.

Historical Review

Paranthropus History and Morphology

The genus *Paranthropus* is an evolutionary oddball, with its three species exhibiting large cranial and dental features argued early on to be adapted for specialized dietary behaviors. The holotype specimen of *Paranthropus robustus* (TM 1517) described by Broom (1938) exhibited a skull larger than an ape, a flat face, and large postcanine teeth almost double the size of teeth in *Homo*. Rak's (1983) comprehensive work detailing the the morphology of the face in early hominin species further explains the large muscular attachments for the masticatory muscles and the facial buttressing seen in *Paranthropus* that is argued to reinforce sections of the face during chewing (Strait et al. 2009, Strait et al. 2010). The dentition of *Paranthropus* is characterized by its postcanine megadontia. The premolars are molarized and the molars have low, bunodont cusps and are large in size (Broom 1938; Robinson 1954b; Rak 1983). These big, flat teeth are seen in primates that consume harder objects and are used to crack the outer casing of objects and grind up foods (Kay 1985; Lucas et al. 1984; Strait 1993).

While Kromdraai yielded the type specimen of *Paranthropus robustus*, there are several prolific sites that also have produced fossils. Subsequent discoveries at the site of Swartkrans were originally named *Paranthropus crassidens,* and they exhibited the similar robust teeth and jaws to *P. robustus* at Kromdraai, but were argued to be a larger morph (Robinson and Broom 1952; Grine 1988). Broom (1938) thought initially that the South African hominins consisted of three separate genera divided into five species, with the two *Paranthropus* species from Kromdraai and Swartkrans separated into *P. robustus* and *P. crassidens*, respectively. This was reassessed by Robinson (1954a) who recognized two genera, *Australopithecus* and

Paranthropus, while additionally maintaining a subspecies distinction between *Paranthropus robustus robustus* (Kromdraai) and *Paranthropus robustus crassidens* (Swartkrans) (Grine 1981). A morphometric analyses of crania from Kromdraai and Swartkrans by Cofran and Thackery (2010) was unable to conclusively determine differences between the two sites. In total, there are five South African sites that have yielded *P. robustus* fossil material: Kromdraai, Swartkrans, Drimolen, Gondolin, and Cooper's Cave.

Looking to evolutionary relationships, arly phylogenetic assessments of the South African material placed *Au. africanus* as the stem hominin, with *Homo* and *Paranthropus* diverging into separate lineages (Johanson and White 1979). With the discovery of *Australopithecus afarensis,* Johanson and White (1979) argued that *Au. africanus* is ancestral to the "robust" lineage based on similar craniodental adaptations, while *A. afarensis* was considered ancestral to *Homo* (Kimbel et al. 1998). The discovery of *P. aethiopicus* further complicated matters. The "Black Skull "(KNM-WT 17000) shares cranial features with *P. boisei*, including its incredibly large size and dished midface (Walker et al. 1986; Suwa et al. 1997; Kimbel et al. 1998). *Paranthropus aethiopicus* is the purported ancestral taxon that gives rise to the two later forms, the eastern African *Paranthropus boisei* and the South African *Paranthropus robustus* (Walker et al. 1986; Strait et al. 1997; Suwa et al. 1997; Kimbel et al. 1998). While there is evidence that *Paranthropus* is a monophyletic clade (Strait et al. 1997), some scholars disagree about the placement of *P. aethiopicus* in relation to the other two species (Skelton and McHenry 1998). This phylogenetic relationship becomes significant when looking at the diets of each species in comparison to the morphological adaptations seen in their masticatory system and dentition.

Dietary Hypotheses and Ecology of Paranthropus

As already mentioned, the cranial, facial, and dental adaptations of the genus

Paranthropus were originally considered to be adaptations for hard object feeding. Robinson

(1954a, 1954b) proposed a dietary split between *Australopithecus* and *Paranthropus*, where the

former was an omnivore and the latter a strict herbivore (Grine 1981). However, cave sites in

South Africa have several examples of hominins being prey to large bodied carnivores, calling

into question the hypothesis that early hominins (specifically species of *Australopithecus*) were

hunters (Grine 1981; Brain 1981). Then, Jolly (1970) proposed a model of hominin evolution

based on seed predation, where the large, flat molars of *Paranthropus* were thought to have

evolved to facilitate grinding small hard seeds. Grine's (1981) work on the trophic differences

between *Au. africanus* and *P. robustus* concluded that both were primarily vegetarian, with *P.*

robustus consuming the harder, more fibrous objects. Work done by Lucas et al. (1984) point to

a relationship between increasing tooth size and the amount of abrasives in food items. They

conclude that the diet of *P. robustus* consists of small, hard objects like seeds as well as fibrous

objects like roots. Chipping of the enamel is also seen in hard object feeding animals, but the

chipped areas are polished, further reflecting how the structure of the tooth maximizes the

continued use of the tooth (Constantino et al. 2010). During times of resource stress, animals

will access less preferred objects in order to sustain themselves through lean times, such as

chimpanzees supplementing their frugivorous diet with less appealing leaves (Constantino and

Wright 2009). Specifically with hard objects, this provides a selective pressure for larger teeth

with thicker enamel that is more resistant to cracking and large cranial and facial features that

can withstand forces generated through biting (Lambert et al. 2004; Lambert 2009; Constantino and Wright 2009; Altmann 2009; Strait et al. 2010; Smith et al. 2014).

Additionally, cranial and facial buttressing are argued to be adaptations to withstand stress in the face during mastication, both in *Paranthropus* and in *Au. africanus* (Rak 1983; Strait et al. 2007; Strait et al. 2008; Strait et al. 2010). Finite element analysis on the face of *Macca fascicularis* and *Au. africanus* suggest to Strait et al. (2009) that the architecture of their faces are adapted to withstand force generated by biting hard objects on the premolars, possibly to exploit harder fallback foods. Sagittal cresting in male specimens and large, deep mandibular corpora also indicate that large masticatory muscles that can generate large amounts of force (Rak 1983).

These adaptations for hard object feeding have been characterized as an adaptive response to a changing environment. Whereas the genus *Homo* broadens their dietary niche with tools and the incorporation of animal protein, *Paranthropus* was characterized as branching off into more stenotopic adaptations, specializing in hard object feeding in response to increasing aridity (Wood and Strait 2004). Grine (1981) explains the differentiation between *Au. africanus* and *P. robustus* in a similar fashion, with more xeric environments driving adaptations for molar morphology better at crushing objects, while molars adapted for shearing are better for mesic environments. Lucas et al. (1984) also highlight the distinction between *Homo* and *Paranthropus* using dietary distinctions. While the euryotopic dietary adaptations of *Homo* facilitated more group sharing and the acquisition of higher quality foods, like meat, *Paranthropus* diverged in the opposite direction, developing a large masticatory apparatus to process low quality items. This characterization of *Paranthropus* provides an image of a genus of early hominin that specialized to consume harder, lower quality foods, and this eventually led

11

to its extinction while the genus *Homo* was better able to adapt because of its dietary flexibility (Potts 1998; Wood and Strait 2004)

However, dietary studies incorporating microwear analysis and stable isotope analysis paint a different picture of dietary and ecological adaptations for *Paranthropus*, especially when examining the eastern African *P. boisei*. Carbon isotopic evidence for early hominins reflect a mixed C_3/C_4 signature (Ungar and Sponheimer 2011). Specifically looking at the C^{14} evidence for *P. robustus*, Sponheimer et al. (2006) see more variation among the carbon signatures, indicating a more variable diet. C_3 plants include plants associated with browsing and more closed environments, while C_4 plants involve more grasses, though there are C_3 grasses and other C_4 plants (Sponheimer et al. 2007). Overall, there is a general trend during the Plio-Pleistocene of increasing incorporation of C_4 resources into the hominin diet (Lee-Thorp et al. 2007; Lee-Thorp et al. 2010). However, South African early hominins have a mixed C_3/C_4 carbon isotope signatures, with *P. robustus* sharing a similar mixed diet to *Au. africanus*, with some evidence for short term changes in diet, either seasonal or yearly (Sponheimer et al. 2006; Ungar and Sponheimer 2011). There is also evidence to suggest that there were seasonal changes to diet, so far as plants with different photosynthetic pathways goes, among *P. robustus* individuals (Sponheimer et al. 2006). This mixed signature is quite different from P. boisei in eastern Africa, which has an almost exclusively C_4 diet that possibly incorporates sedges and C_4 herbs (Sponheimer et al. 2005; Sponheimer et al. 2006; Cerling et al. 2011).

Microwear studies have also been utilized to piece together the diet and behavior of fossil hominins, and a review of dental microwear studies is provided below.

Dental Microwear and Dietary Analysis

The earliest microwear studies focused on the relationship of chewing movement and the striations left on the enamel from the movement of food across the occlusal surface (Simpson 1933; Butler 1952; Mills 1955). Baker et al. (1959) further looked at sheep microwear and proposed that it was caused by a combination of chewing and the phytoliths and exogenous grit on the foods themselves. It was not until Dahlberg and Kinzey (1962) examined a sample of human teeth with a low-magnification light microscope that microwear was applied to questions in Anthropology, however. Their conclusions highlighted the importance of food particles per se in forming scratches in enamel. Later researchers further explored microwear with other mammal groups and fossils, while also incorporating more advanced technology (see Rose and Ungar 1998, for review).

The first advanced technology used in microwear analysis was scanning electron microscopy (SEM). The SEM bombards the surface of an object with electrons in order to produce high resolution, two-dimensional images. This technology was a great asset to microwear studies, as microwear features were easily distinguished on the surface images and could then be quantified. However, initial SEM microwear studies were mostly qualitative in natures (Walker 1981; Grine 1981). Early attempts to quantify features required hand counting and measuring of features (Grine 1986; Walker and Teaford 1989). Semi-automated attempts to standardize quantification methods facilitated comparisons among researchers, but observer measurement error was still an issue (Ungar 1995; Grine et al. 2002). Nevertheless, numerous studies did have success using SEM scans to assess differences among both australopiths and members of *Homo*. Studies of *A. afarensis* anterior dental microwear reflected a similar pattern

of features to both baboons and gorillas, suggesting that they were stripping leaves using their incisors (Ryan and Johanson 1989). Ungar and Grine (1991) compared incisor microwear patterns of *Au. africanus* and *P. robustus*, showing higher concentrations of wear striations in the former, leading to the conclusion that the larger incisors of *Au. africanus* made it able to process more large, perhaps abrasive items than *P. robustus*. Concerning molar microwear, as already mentioned, SEM micrographs show that *Au. africanus* has a higher predominance of scratches on its surface, while *P. robustus* has more pitting, suggesting that the later ate more hard objects (Grine 1986). Feature-based SEM microwear studies on *A. afarensis* and *A. anamensis* also show utilization of occasional hard object fallback foods for *A. anamensis*, but that neither of their diets appeared in any way dominated hard object feeding (Grine et al. 2006; Ungar et al. 2010).

Hominin studies utilizing microwear analyses also reflect a more complex relationship between the morphology of *Paranthropus* species and its actual diet. Initial studies of the deciduous cheek teeth of "gracile" and "robust" species of *Australopithecus* point to a fundamental difference between *P. robustus* and *Au. africanus* diets. *Australopithecus africanus*, the more "gracile" of the South African hominin species, was suggested to have a microwear pattern dominated by parallel striations, which was attributed to grinding softer, tougher foods. In contrast, *P. robustus* has a more pitted surface texture associated with crushing hard objects (Grine 1981). A follow-up study of permanent molars using scanning electron microscopy by Grine (1986) further explored microwear textures on a sample of $n = 9$ *P. robustus* individuals. Grine found a higher rate of pitting than seen in a sample of $n = 10$ *Au. africanus* specimens. The features observed on *P. robustus* teeth were on average shorter but wider than those found on

Au. africanus teeth; and they were found on both the Phase I and Phase II facets, which occur when the tooth comes into occlusion at different parts of the chewing cycle (Grine 1981; Krueger et al. 2008).

Scott et al. (2005) later applied dental microwear texture analysis (DTMA) using scale sensitive fractal analysis to compare the same specimens of South African hominin as Grine (1986), both to one another, and to a sample of modern *Cebus apella* and *Alouatta palliata* individuals. For DMTA analysis, higher complexity values seem to correspond to higher degrees of hard object feeding, while anisotropy values are often found in tough object eaters (Scott et al. 2006; Scott et al. 2012). Scott et al.'s (2005) interpretations were consistent with those of Grine (1986). *Australopithecus africanus* was still said to have predominance of scratches, as suggested by low complexity and higher anisotropy averages, which again was proposed to imply a diet including some tough foods. In contrast, *P. robustus* has higher average complexity and lower anisotropy on average, consistent with more pitting on its surface and the consumption of more hard objects. In addition, Scott et al (2005) underscored the overlap between these two species in microwear complexity and anisotropy, and suggested that the distribution of data (i.e., the dispersion) is important for interpreting food preferences and foraging strategies. Specifically, they suggested that these two hominins likely had overlapping diets, but "fell back" in different directions, with *P. robustus* supplementing their diets with more hard foods, and *Au. africanus* consuming more tough ones, consistent with differences in occlusal morphology (Ungar, 2007). That said, the microwear samples used by Scott et al. (2005) were small, with a total sample size for *P. robustus* being *n* = 9 and the total for *Au. africanus* of *n* = 10.

Further complicating the dietary picture for *Paranthropus,* the microwear textures for a sample of *n* = 7 specimens of *P. boisei* exhibited no evidence for hard object feeding, appearing to directly contradict conclusions drawn from the species robust "Nutcracker" morphology (Ungar et al. 2008). In this instance, if *P. boisei* is "falling back" on hard objects, that feeding behavior is not seen in the microwear textures. This implies that if *P. boisei* is relying on hard objects as a fallback resource, it is inhabiting an environment where it does not engage in fallback food use often enough to leave a microwear pattern on the teeth. This is distinctly different from the textures seen in *P. robustus*, which has a pattern similar to primates that consume hard objects as fallback resources (Scott et al. 2005). An additional interpretation involves the use of suboptimal resources. The large, flat molars of *P. boisei* are not an ideal platform for consuming tougher resources, but are an exaptation useful for repetitive grinding of vegetation (Bock and von Wahlert 1965; Ungar and Hlusko 2016). This would explain both the presence of a large morphology, possibly originally adapted to hard object feeding, and the isotopic and microwear signatures.

However, with such small samples in analyses for both species of *Paranthroups*, it is possible that these data are not representative of the species as a whole. Increasing the sample size would allow for more robust statistical analyses, as well as incorporate more sites, which has the potential to increase the variation among the total sample. In this context, it is important to understand site contexts and what they can tell us about food availability to the individuals represented in the samples.

The current method of DMTA analysis was developed because of the measurement error and the time and expense inherent to SEM-based studies. The DTMA approach uses three-

dimensional point clouds to represent the topography of the enamel surface and scale-sensitive fractal analysis (SSFA) for a quantitative characterization of that topography. Various aspects of the surface roughness, including size, shape, and depth of features both across the surface and at varying scales (Ungar et al. 1991; Ungar et al. 2003; Scott et al. 2006). While individual texture measures are largely automated, reducing observer measurement error, researchers still require training to distinguish antemortem microwear from taphonomic artifacts.

This study endeavors to expand the microwear baseline previously done by Scott et al. (2005). With an expanded sample, this increases the chance of sampling a wider array of behaviors than previously. If *P. robustus* has a wider range of dietary behaviors than what is seen sampled by the previous study, this larger sample should exhibit more variability in textures. This variation in microwear textures would also be seen if there were differences among samples from different deposits.

Materials and Methods

Samples and Casting Procedure

All microwear replicas were created from dental impressions of *P. robustus* molars taken from original specimens by Peter Ungar, Fred Grine, Mark Teaford, and Alejandro Pérez-Pérez in the collections of the Ditsong Museum in Pretoria and the University of the Witwatersrand in Johannesburg. Teeth were first cleaned with acetone-soaked cotton swabs, then molds were prepared with President's Jet regular body polyvinylsiloxane material (Coltene-Whaledent Corp.). All available permanent molars attributed to *P. robustus* in both collections were molded.

The Swartkrans material makes up the bulk of the analyzed sample with a total of 93 specimens available, representative of four different stratigraphic deposits: Member 1 Hanging Remnant, Member 1 Lower Bank, Member 2, and Member 3. These newly sampled specimens were added to the original *n* = 9 used by both Grine (1986) and Scott et al. (2005). The Drimolen sample makes up the other significant portion of the specimens with a total of 22 individuals available for analysis (following Moggi-Cecchi et al. 2010). The Kromdraai sample consists of 6 specimens. Resulting data were compared with those for an enlarged sample of *Au. africanus* (*n* = 44) from both Sterkfontein and Makapansgat collected by Elicia Abella.   The *Au. africanus* sample is presented and analyzed here for comparison with the *P. robustus* data collected for this thesis (see Appendix Tables 1 and 2).

Microwear quality replicas were made using high-resolution epoxy resin (Epoxy Technologies Corp.). Epoxy was poured into prepared molds and then the mold is spun in a centrifuge to remove air bubbles from the surface. Remaining casting material was added to the

molds using a pipette to minimize air bubble creation. Casts are then allowed to cure for twenty-four hours before being carefully removed from the molds.

Site Context

 The specimens examined in the current study come from the sites of Kromdraai, Swartkrans, and Drimolen. The contexts of each of these sites are summarized here.

Kromdraai

 The site of Kromdraai has two main deposits - Kromdraai A and Kromdraai B. While Kromdraai A has a larger sample of mammalian remains, all hominins derive from Kromdraai B (Vrba 1981). These two deposits appear to have been deposited at different times (Brain 1981). McKee et al. (1995) suggest that both Kromdraai A and B are quite similar, but due to the presence of *P. robustus* in the assemblage, Kromdraai B may be slightly older, though both are suggested to be deposited prior to Swartkrans Member 1. Alternatively, Herries and Adams (2009) argue that the faunal assemblage at Kromdraai A is contemporaneous with Member 1 at Swartkrans and has a reconstructed age range of 1.89 to 1.63 mya based on the age ranges of species. Kromdraai B has undergone several studies to assess its dating, as the context is crucial to the hominin fossils found in this deposit. Biochronological assessments of the faunal assemblage of Kromdraai B are more difficult as there are less time sensitive taxa present than in Kromdraai A (McKee et al. 1995; Herries and Adams 2009). Paleomagnetic dating of the context of TM 1517 are consistent with a date of 1.9 mya (Thackeray et al. 2002).

Assessments of the sedimentological context of Kromdraai B indicate a higher average annual rainfall than today at the site, which is supported by the presence of *Hippopotamus* and wet adapted micromammals (Brain 1958; Partridge 1985; Vrba 1981). The site also has an abundance of primate and large bodied carnivore remains (Vrba 1981). Given that the number of woodland adapted fauna are greater than the grassland adapted fauna, de Ruiter et al. (2008) concluded that Kromdraai had more woodland, with the site being fed by the Blaaubank River as a permanent water source, though it did likely have some grassland components (Vrba 1981). de Ruiter et al. (2008) hence argued that *P. robustus* was exploiting both the grassland and the woodland, making it an environmental generalist. The micromammalian record also indicates the presence of both forested and grassland adapted species (Avery 1995).

Kromdraai's paleoenvironment is different from many of the other South African sites given its higher rainfall and larger component of riparian forest (de Ruiter et al. 2008; Vrba 1981). That said, not all studies are consistent with a forest setting. Pollen studies suggest more open adapted vegetation (Carrion and Scott 1999).

Swartkrans

The nearby site of Swartkrans has produced the largest sample of *P. robustus* fossils, with material coming from several distinct stratigraphic units. The most fossiliferous deposit is Member 1, which is divided into the Hanging Remnant and the Lower Bank. The Hanging Remnant is attached to the northern wall of the cave, while the Lower Bank is made up of more sandy and decalcified sediment that is separated from the Hanging Remnant (Brain 1989; Brain 1993a; Brain 1993b; Gibbon et al. 2014). The site was initially excavated by Broom and

Robinson, and the bulk of the *P. robustus* material comes from Member 1 Hanging Remnant (Brain 1981). Smaller samples of *P. robustus* also derive from the Lower Bank as well as Members 2 and 3.

While early reconstructions of Member 1 inferred the paleoenvironment to have been open savannah, Reed (1997) reconstructed a more closed to mixed habitat using the morphological characteristics of fossil fauna. *Paranthropus* was said to inhabit similar a mix of more closed settings and open grasslands. de Ruiter (2003) also examined the faunal record for Member 1, concluding that Members 2 and 3 are roughly contemporaneous, being dated to approximately 1.6 mya, and also representative of a more closed, forested environment. On the other hand, isotopic studies show a general trend toward more C_4 plants in the diets of present fauna, indicative of a more open grassland (Lee-Thorp et al. 2007). In Member 2, the faunal assemblage also reflects a mixed environment, with a dedicated water source or wetland area being common to several reconstructions (Reed 1997; de Ruiter 2008; Avery 2001). The Member 3 habitat has been reconstructed to be similar to Members 1 and 2 (Reed 1997). Interestingly, Brain and Shipman (1993) note the presence of bone tools, presumably used for digging or hide preparation.

Drimolen

Drimolen is further north than both Kromdraai and Swartkrans and was discovered in 1992 by Andre Keyser, yielding a number of *P. robustus* remains and a large number of faunal remains from the Main Quarry (Keyser 2000; Keyser et al. 2000; Moggi-Cecchi et al. 2010). Among the faunal remains, Drimolen has a lower incidence of porcupines and hyraxes than other

South African sites while having unique single occurrences of giraffe, elephant, and aardvark. Despite this diversity, there are no ecologically specific species that are distinctly different from other karst sites (Adams et al. 2016). Time specific macromammalian species indicate the site represents a period of time from 2.0-1.5 mya, though it was possibly deposited as early as 2.33 mya, based on the presence of *Equus* in the deposit (Keyser et al. 2000; Adams et al. 2016).

Of particular note are both the large presence of *P. robustus* individuals as well as a large sample of other primate fossils that represent 554 specimens (Adams et al. 2016). There are, in addition, a number of carnivore specimens, specifically Felidae, that are comparable to those from other South African sites, though the sabertooth *Dinofelis* appears to represent a more primitive form (Adams et al. 2016; Rovinsky et al. 2015). The nearby Makondo deposit is about 55 meters west of the Main Quarry and, while there is some overlap among the macromammalian record of both deposits, there is a higher proportion of hyaenid and canid remains, in addition to more carnivore-related taphonomic damage on the other fossils. The Makondo deposit unfortunatley lacks the biochronologically distinct taxa necessary to estimate an age range for the site (Rovinsky et al. 2015). Like Swartkrans, Drimolen has a record of bone tools and termite foraging (Backwell and d'Errico 2001; Backwell and d'Errico 2008).

DMTA Scanning Protocol

Replicas were examined for microwear using a white light confocal profiler and Sensofar PLm imaging software (Solarius, Inc.). Three dimensional point clouds are generated of areas on the Phase II chewing facets of each molar, which provide dietary signals (Kay 1977; Krueger et al. 2008). Scanning preference was for facet 9 on the second molars, consistent with protocol

used in the original microwear studies (Grine 1986; Scott et al. 2005). In the case where second molars are unavailable, or if microwear is not preserved or is taphonomically altered, first and third molars were used. Where facet 9 was not preserved, the surface did not preserve microwear, or the surface is taphonomically damaged, facet 10n is used. There is no demonstrable difference in microwear signatures between facet 9 and facet 10n, or among tooth types (e.g., maxillary or mandibular first, second, or third molars). In addition, specimens that do not preserve antemortem microwear on any Phase II facet were excluded from analysis (see below).

The occlusal surface was leveled on the stage of the confocal profiler so the facet to be sampled was parallel to the plane of the base. An area representative of the pattern seen on the entire facet surface and is free from casting defects or taphonomic damage was selected. Imagery from the original Scott et al. (2005) study was used as a guide for site selection. All taphonomically altered specimens are removed from the study sample prior to analysis. Studies by King (1999) and Teaford (1988) have found that surfaces damaged due to taphonomic processes, such as acid etching, are demonstrably different in appearance from surfaces that preserve microwear created through dietary behaviors. While taphonomic damage can often be confused for microwear features, the damage is often clearly identifiable, as taphonomic processes impact the surface of the whole tooth and is not limited to wear facets (King 1999). This kind of pattern can produce what appears to be a surface-wide texture that acts like a film over the microwear, or obscures/obliterates the microwear entirely.

Once an appropriate surface has been identified, four adjacent scans of 138 x 102 mm were made, with a lateral point spacing of 0.18 mm, a vertical step of 0.2 mm, and a resolution of

<5 nm. This means a total sampled area of 276 x 204 mm for each tooth surface. When the four scans are generated, any small defects on the surface can be erased digitally using MountainsMap software (Digital Surf). Removed areas are registered as non-measured points, and do not impact the scale-sensitive fractal analysis (SSFA) protocols.

Because specimens that do not preserver antemortem microwear were removed from the study before analysis, this greatly reduced the number of specimens analyzed. There were the total of $n = 93$ specimens available to scan. The largest sample came from Swartkrans Member 1 Hanging Remnant, in which $n = 42$ available specimens preserved microwear, including the original $n = 8$ previously scanned from the deposit. From Swartkrans Member 1 Lower Bank, $n = 6$ specimens preserved microwear, while $n = 3$ came from Member 2, and $n = 1$ came from Member 3. The Kromdraai sample also had a small sample size of $n = 5$, including the single specimen from the site included in previous microwear studies. The Drimolen sample consisted of $n = 12$ specimens.

Scale-Sensitive Fractal Analysis

Scans are then processed using Toothfrax and Sfrax analytical software programs. Scale-sensitive fractal analysis uses fractal geometry to assess the texture of a surface, considering areal, length, and volume at varying scales of observation. At a coarse scale, a surface may appear to be relatively smooth, but upon closer inspection shows a rough, uneven surface (Scott et al. 2006; Brown and Seigmann 2001). Five SSFA texture variables were used in this study, following convention for microwear texture analysis.

Complexity, or Area-scale fractal complexity (*Asfc*), is the measure of the changes in roughness over the surface at a given scale. A virtual tiling algorithm uses different sizes of triangles to fill in the surface at increasingly finer scales, from 7200 mm² to 0.02 mm². The steepest part of the slope is then fit to a log-log plot that places relative area over range of scales, and is then multiplied by -1000 (Scott et al. 2006). Simply put, complexity values are indicative of the change of roughness on a surface with scale of observation. In previous studies, hard object feeding primates have been suggested to average higher complexity values, indicating microwear features that vary in both size and shape (Scott et al. 2005; Scott et al. 2006). Scale of maximum complexity (*Smc*) is the steepest part of the complexity curve and represents the finest scale at which the surface is most complex (Scott et al. 2006). High *Smc* values reflect larger microwear features seen at coarser scales.

Exact proportion length-scale anisotropy of relief (*epLsar*) measures the orientation of texture across the surface. The relative lengths of line segments at different scales measured at different directions vary if there is a distinct directionality to surface texture (Scott et al. 2006). A highly anisotropic surface consists of regular features oriented in the same way, such as many parallel striations. A surface with lower anisotropy values tends to lack this directionality. This high anisotropy is seen in primate samples that incorporate tougher foods into their diets (Scott et al. 2005, Scott et al. 2006).

Textural fill volume (*Tfv*) measures surface volume and is calculated by filling in features with cuboids of two and ten microns in diameter. The difference in volume between the two cuboid sizes sampled can provide information about feature size (Scott et al. 2006). The higher the relative volume of cuboids, the more features in the range between 2 - 10μm in diameter. In

this sense, large *Tfv* values may be seen with hard object feeding, as the harder objects are pressed into the occlusal surface of the tooth and deform or carve out the enamel (Scott et al. 2006).

The final variable is heterogeneity of area-scale fractal complexity (*HAsfc*), which measures how much variation is present in complexity (*Asfc*) across the surface. Each scan is divided into a grid made of equal numbers of rows and columns that increase in number until an 11 x 11 grid is formed. Complexity is subsampled from each grid, and *HAsfc* is defined as heterogeneity in *Asfc* across subsampled areas. The heterogeneity values used most frequently in microwear analyses are 3x3 (*HAsfc9*) and 9x9 (*HAsfc81*).

Additionally, International Organization for Standardization (ISO) parameters (ISO 25178-2) were incorporated into this study, as these are becoming increasingly popular for microwear texture characterization. There are ten ISO variables commonly used in microwear texture analysis today to detail parameters that assess different aspects of roughness (Calandra et al. 2012; Purnell et al. 2012; Schulz et al. 2013; Delezene et al. 2016). ISO variables considered here and their descriptions are listed in Table 1.

Table 1: ISO values used in this study, with a brief description.

Parameter	Desctiption	Type of Parameter
Ssk	Skewness	Height
Sp	Maximum Peak Height	Height
Sz	Maximum Height	Height
Sxp	Extreme Peak Height	Functional
Sdq	Root Mean Square Gradient	Hybrid
Sdr	Developed Interfacial Area Ratio	Hybrid
Vvv	Pit Void Volume	Functional (Volume)
S5v	Five Point Pit Height	Feature
Sda	Mean Dale Area	Feature
Sdv	Mean Dale Volume	Feature

ISO measurements were made using MountainsMap (Digital Surf) software. Individual point clouds required further processing prior to analysis for ISO attributes because these measurements are affected by overall surface form and missing data. As such, surface form was removed using the default polynomial of order 5<13 to adjust for facet shape, and missing data were filled using a nearest neighbor algorithm in MountainsMap following standard protocols.

Soft Filter Protocol

A soft filter protocol was also applied prior to both SSFA and ISO data collection, following that developed by Arman et al. (2016). This soft filter is designed to mitigate comparability issues among confocal instruments. One of the principal goals of microwear texture analysis is comparability of results among studies and the development of a large database to which fossils of numerous taxa can be compared with one another and with data for

extant species. Arman et al. (2016) found variation in results obtained for the same specimens

when using different instruments in different laboratories. Indeed, even instruments with

comparable specifications can provide lead to somewhat different results given varying

tolerances for data spikes, light source intensity, objective characteristics, etc. That said, soft-

filtering applied to a surface in MountainsMap (Digital Surf) removes outliers, removes form,

and fills in non-measured points to reduce measurement "noise" introduced by the vagaries of

individual instruments and results in more comparable surfaces. The soft filter was applied to

the raw data files prior to being run through the Toothfrax and Sfrax software and before

generating ISO values. Soft filtered results are the median values of the four sampled areas,

which is the same as other microwear studies. Results reported are the soft filtered data results,

seen in Appendix tables 1 and 2. A complete list of all specimens available for this study is also

reported in Appendix table 3.

Statistical Protocol

General linear models were used to assess differences between *Au. africanus* and *P.

robustus*, and differences among *Paranthropus* samples from the various deposits. Separate

protocols were used to assess variation in central tendencies and variation in distribution

dispersion among samples using Systat 12. The single specimen from Swartkrans Member 3,

SKx19892, was not included in comparisons between deposits given that n =1 is not amenable

to analyses of variance.

Central tendencies were assessed following rank transformation to mitigate effects of

violation of assumptions inherent to parametric statistics (Conover and Iman 1981). ISO and

SSFA attributes were considered together for both the between species and between deposit

models. MANOVAs were used to determine/establish significance in the models (i.e., whether

the samples differed in their microwear textures), and individual ANOVAs were used to

determine the sources of significant variation as necessary (i.e., how the samples differed in their

microwear textures).

To determine whether the species differed in dispersion, conventional pairwise two-

sample variance tests were used on each of the variables considered in this study. For

assessment of dispersion variation among the sites, both Bartlett's and Levene's equality of

variance tests were used. Additional pairwise two-sample variance tests were used to assess the

sources of significance (i.e., which pairs of deposits differed from one another in texture

dispersion for specific variables). It should be noted that the number of tests included here does

make Type I errors possible. However, experiment-wide error rates were not used, as this would

surely increase Type II errors (Perneger 1998).

Results

A total of 66 out of 93 specimens examined yielded microwear data. The largest sample comes from Swartkrans Member 1 Hanging Remnant with $n = 33$ specimens preserving microwear, bringing the total known sample of microwear from the Hanging Remnant to $n = 41$. The Lower Bank sample yielded $n = 5$, while Member 2 yielded $n = 3$ and Member 3 yielded $n = 1$. Because Member 3 only had a single individual preserve microwear, the statistical analyses will not include the Member 3 specimen (SKX 19892). For Kromdraai, $n = 4$ specimens yielded microwear. Drimolen yielded $n = 12$. Descriptive statistics for SSFA and ISO data are presented in Tables 1-2, along with a comprehensive list of all the *P. robustus* specimens used and which ones yielded microwear in Appendix Table 1. All scans have surfaces that has a combination of pits and scratches and representative scans from each deposit are depicted in Figures 1-5.
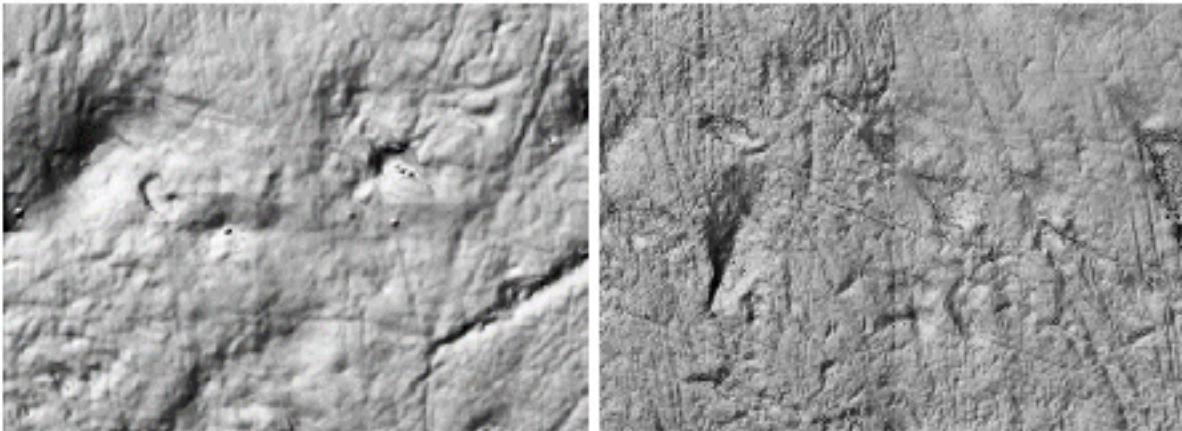
Figure 1: Photosimulations of two specimens from Drimolen: DNH 22a (Left) and DNH 3 (Right).
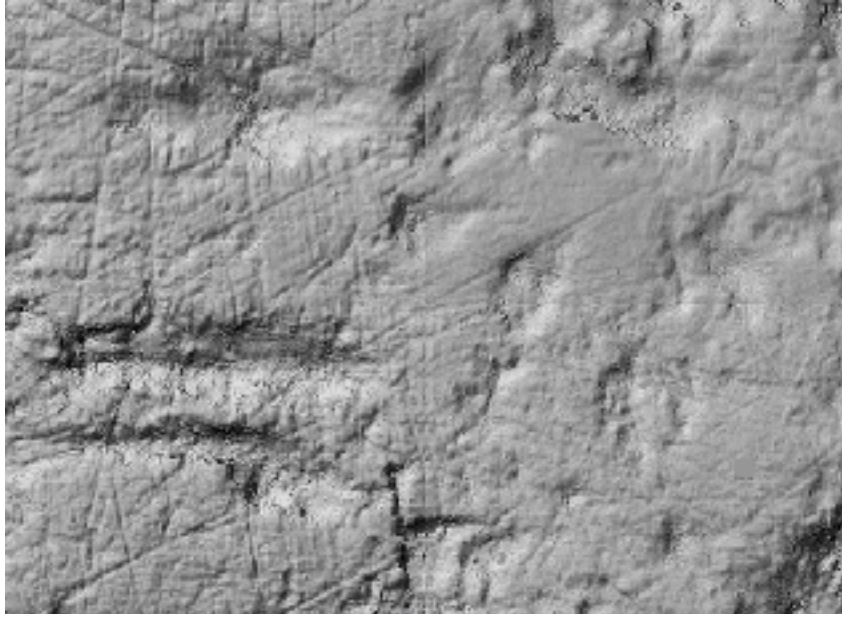
Figure 2: Photosimulation of a specimen from Kromdraai: KB 5222.

Figure 3: Photosimulation of a specimen from Swartkrans Member 1 Hanging Remnant: SK 52.

Figure 4: Photosimulation (Top) and 3D topographic image (Bottom) of a specimen from Swartkrans Member 1 Hanging Remnant: SK 31.
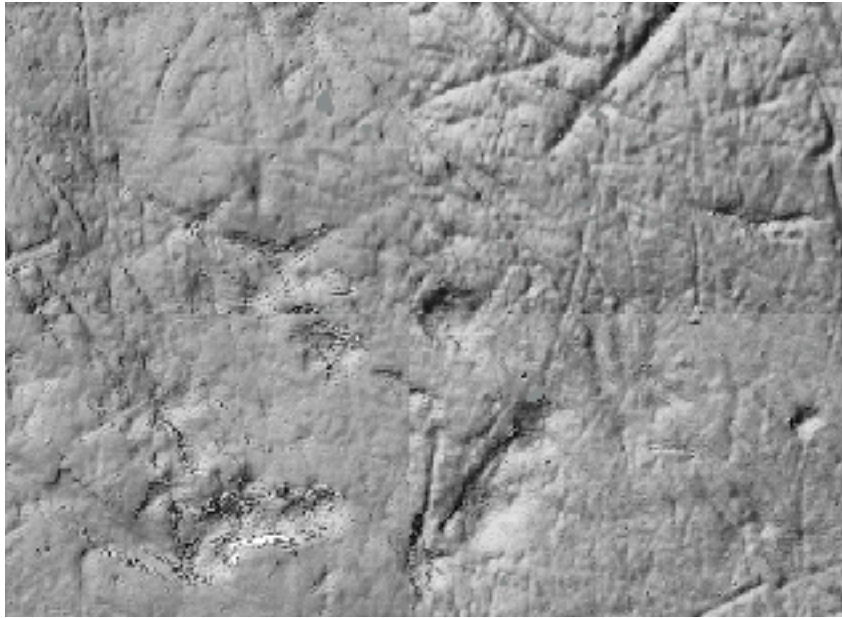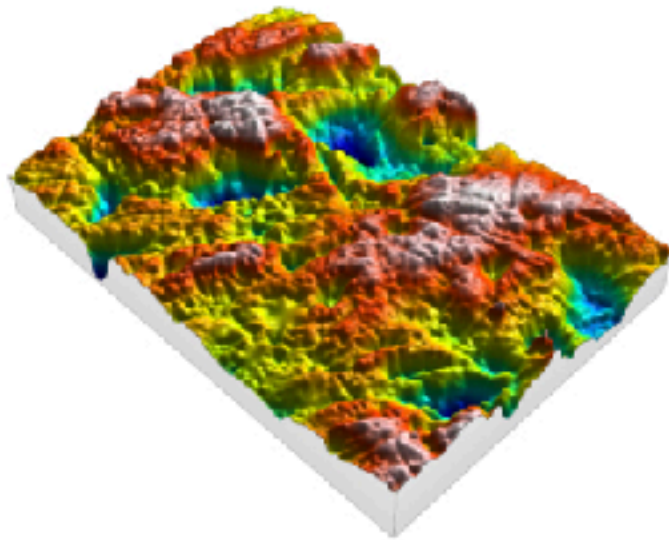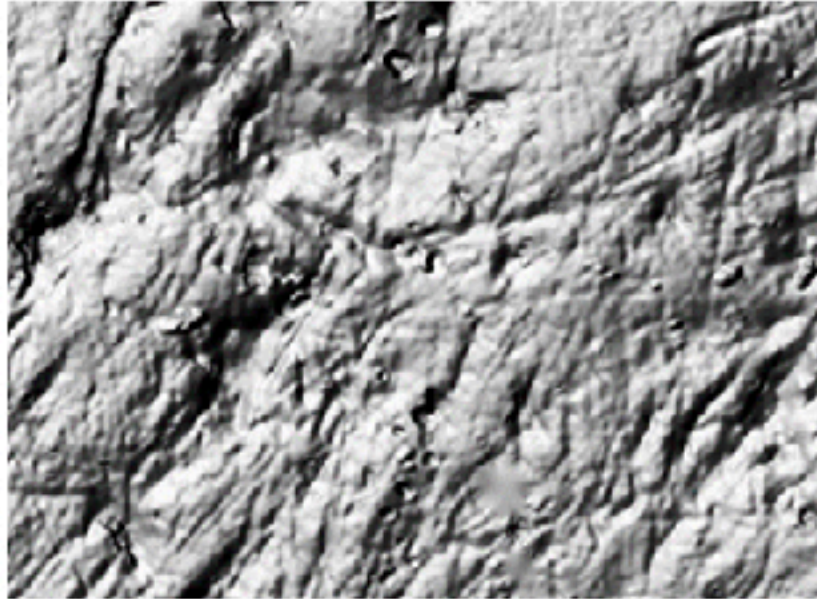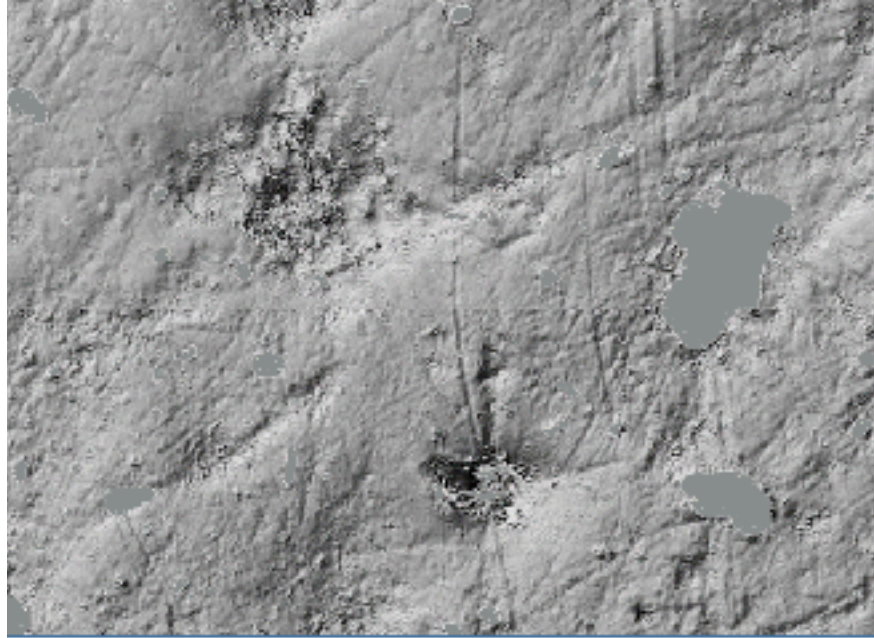
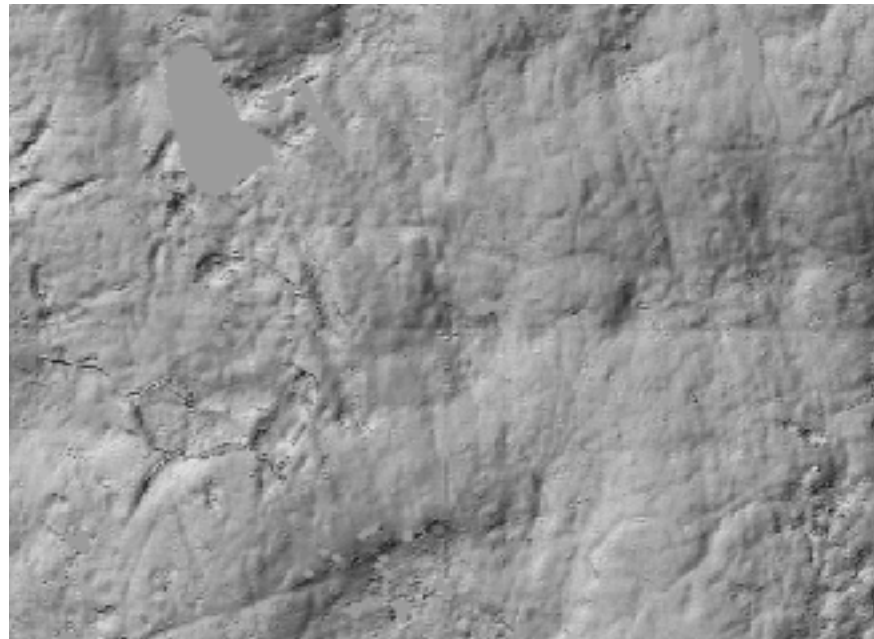Figure 5: Photosimulation of a specimen from Swartkrans Member 1 Lower Bank: SKX 5014.

Figure 6: Photosimulation of a specimen from Swartkrans Member 2: SKX 4446.

Table 2: Scale-sensitive fractal analysis descriptive statistics (*epLsar* data reported as x10^{-3})

SSFA Descriptive Statistics

		Asfc	*epLsar*	*Smc*	*Tfv*	*HAsfc9*	*HAsfc81*
P. robustus	*n* = 66						
	Mean	0.957	2.983 x 10^{-3}	9.240	6738.884	0.456	0.797
	Median	0.846	2.743 x 10^{-3}	4.675	6239.505	0.417	0.727
	SD	0.459	1.219 x 10^{-3}	16.782	4752.536	0.180	0.280
Drimolen	*n* = 12						
	Mean	1.126	2.901 x 10^{-3}	17.180	9162.150	0.441	0.760
	Median	1.031	2.683 x 10^{-3}	5.490	9382.899	0.476	0.726
	SD	0.518	1.150 x 10^{-3}	34.634	5170.237	0.135	0.188
Kromdraai	*n* = 4						
	Mean	0.950	2.698 x 10^{-3}	8.095	4132.784	0.625	1.143
	Median	0.948	2.668 x 10^{-3}	8.775	3616.081	0.471	0.901
	SD	0.247	0.279 x 10^{-3}	4.675	2287.666	0.315	0.626
Swartkrans M1 HR	*n* = 33						
	Mean	0.952	3.154 x 10^{-3}	6.088	6250.454	0.439	0.762
	Median	0.834	2.841 x 10^{-3}	3.920	5413.003	0.405	0.713
	SD	0.496	1.377 x 10^{-3}	4.920	4728.558	0.175	0.221
Swartkrans M1 LB	*n* = 5						
	Mean	0.589	2.421 x 10^{-3}	21.266	3947.893	0.537	0.937
	Median	0.652	2.246 x 10^{-3}	9.530	3695.852	0.516	0.642
	SD	0.160	0.579 x 10^{-3}	22.789	1927.569	0.298	0.579
Swartkrans M2	*n* = 3						
	Mean	1.102	2.324 x 10^{-3}	3.897	11388.441	0.402	0.751
	Median	1.091	2.421 x 10^{-3}	3.650	11371.875	0.413	0.829
	SD	0.090	0.183 x 10^{-3}	1.140	5089.983	0.049	0.215

Table 2 (Cont.): Scale-sensitive fractal analysis descriptive statistics (*epLsar* data reported as x10^{-3}).

SSFA Descriptive Statistics

		Asfc	*epLsar*	*Smc*	*Tfv*	*HAsfc9*	*HAsfc81*
A africanus	*n* = 44						
	Mean	0.689	4.527 x 10^{-3}	6.994	2386.292	0.387	0.699
	Median	0.638	3.830 x 10^{-3}	4.500	1208.628	0.360	0.695
	SD	0.307	2.092 x 10^{-3}	7.601	3076.133	0.129	0.162
Makapansgat M3	*n* = 9						
	Mean	0.636	5.319 x 10^{-3}	11.413	2384.671	0.401	0.732
	Median	0.650	3.717 x 10^{-3}	6.370	1501.830	0.401	0.687
	SD	0.149	2.532 x 10^{-3}	10.804	2089.375	0.092	0.120
Sterkfontein M4	n = 35						
	Mean	0.702	4.323 x 10^{-3}	5.858	2386.709	0.384	0.691
	Median	0.573	3.894 x 10^{-3}	4.210	1132.828	0.356	0.696
	SD	0.336	1.954 x 10^{-3}	6.253	3307.601	0.138	0.171

Table 3: International Organization for Standardization texture parameter descriptive statistics.

ISO Descriptive Statistics

		Ssk	Sp	Sz	Sxp	Sdq	Sdr	Vvv	S5v	Sda	Sdv
P. robustus	*n* = 66										
	Mean	-0.601	1.340	3.310	1.255	0.108	0.616	0.077	0.691	520.538	10.383
	Median	-0.580	1.264	3.197	1.156	0.102	0.516	0.071	0.659	505.903	8.817
	SD	0.357	0.477	1.006	0.416	0.028	0.327	0.026	0.252	150.571	6.297
Drimolen	*n* = 12										
	Mean	-0.670	1.500	3.868	1.471	0.117	0.725	0.090	0.781	526.191	9.879
	Median	-0.534	1.505	3.936	1.403	0.112	0.629	0.088	0.745	504.491	9.065
	SD	0.397	0.520	1.238	0.504	0.032	0.389	0.030	0.277	164.516	3.886
Kromdraai	*n* = 4										
	Mean	-1.031	1.063	3.323	1.380	0.111	0.611	0.086	0.798	618.261	15.783
	Median	-0.830	1.011	3.254	1.410	0.110	0.610	0.088	0.634	673.488	15.465
	SD	0.650	0.154	0.444	0.117	0.017	0.175	0.009	0.357	224.043	10.432
Swartkrans M1 HR	*n* = 33										
	Mean	-0.558	1.300	3.161	1.201	0.108	0.618	0.073	0.669	492.361	9.777
	Median	-0.584	1.271	3.114	1.137	0.103	0.534	0.066	0.641	464.859	7.822
	SD	0.312	0.445	0.986	0.415	0.029	0.337	0.027	0.249	137.435	6.549
Swartkrans M1 LB	*n* = 5										
	Mean	-0.600	1.126	2.936	1.080	0.086	0.378	0.067	0.550	653.415	12.687
	Median	-0.649	1.199	3.042	1.012	0.092	0.420	0.065	0.563	696.891	9.999
	SD	0.203	0.177	0.493	0.311	0.013	0.100	0.016	0.135	159.648	7.141
Swartkrans M2	*n* = 3										
	Mean	-0.344	1.974	3.974	1.415	0.118	0.696	0.089	0.767	530.287	8.755
	Median	-0.467	1.811	4.126	1.408	0.123	0.742	0.091	0.715	600.850	8.812
	SD	0.232	0.872	0.868	0.160	0.007	0.082	0.010	0.112	131.111	0.947

Table 3 (Cont.): International Organization for Standardization texture parameter descriptive statistics.

ISO Descriptive Statistics

		Ssk	Sp	Sz	Sxp	Sdq	Sdr	Vvv	S5v	Sda	Sdv
Au. africanus	*n* = 44										
	Mean	-0.606	0.926	2.355	0.900	0.088	0.398	0.055	0.584	461.814	7.906
	Median	-0.467	0.865	2.192	0.856	0.085	0.353	0.053	0.540	433.416	6.483
	SD	0.382	0.313	0.697	0.294	0.020	0.184	0.018	0.204	159.194	5.619
Makapansgat M3	*n* = 9										
	Mean	-0.536	0.966	2.426	0.956	0.088	0.374	0.056	0.606	591.103	6.478
	Median	-0.405	0.872	2.205	0.858	0.087	0.375	0.054	0.499	670.915	6.404
	SD	0.235	0.212	0.485	0.230	0.010	0.083	0.013	0.217	186.808	2.312
Sterkfontein M4	n = 35										
	Mean	-0.624	0.916	2.337	0.886	0.088	0.404	0.055	0.578	428.568	8.274
	Median	-0.467	0.814	2.179	0.806	0.084	0.348	0.051	0.552	406.894	7.004
	SD	0.412	0.336	0.747	0.309	0.021	0.202	0.019	0.203	135.195	6.164

To address concerns about potential differences concerning tooth position and the inclusion of facet 10n, box plots of *Asfc*, *epLsar*, and *Tfv* data for P. robustus results was done by A. Peterson and a three-factor MANOVA examining tooth number (first, second, and third molars) and jaw (maxillary and mandibular) was done by P. Ungar on the Swartkrans Member 1 Hanging Remnant and Sterkfontein Member 4 samples (Table 4). There are no significant effects with either tooth number or jaw. The only significant effect was taxon. This means there is no significant difference among different teeth in the mouth. Additionally, the boxplots (Fig. 7) shows that the use of facet 10n as a Phase II facet provides the same information as facet 9, confirming what was also seen in a study of Phase I and Phase II facets by Krueger et al. (2008).

Table 4: Three-factor MANOVA comparing tooth types by site/taxon. Results reported for rank-transformed SSFA data (variables), jaw (maxillary, mandibular), tooth number (first, second, third molar), and site (Sterkfontein Member 4, Swartkrans Member Hanging Remnant).

MANOVA Results for Tooth Types

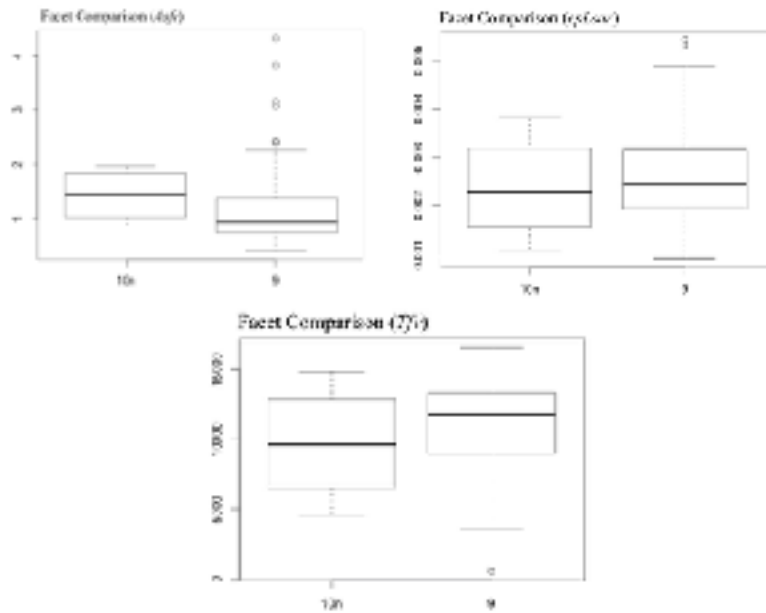| Effect	Wilk's λ	F-ratio	df	p-value
Jaw	0.986	0.156	6, 68	0.987
Tooth number	0.841	1.024	12, 136	0.431
Site (taxon)	**0.737**	**4.035**	**6, 68**	**0.002**
Number x site	0.928	0.434	12, 136	0.947
Jaw x site	0.972	0.323	6, 68	0.923
Number x jaw	0.839	1.042	12, 136	0.414
Number x jaw x site	0.820	1.185	12, 136	0.300

Figure. 7: Boxplots showing the comparison of facet 10n and facet 9 for P. robustus specimens for the variables Asfc, epLsar, and Tfv.
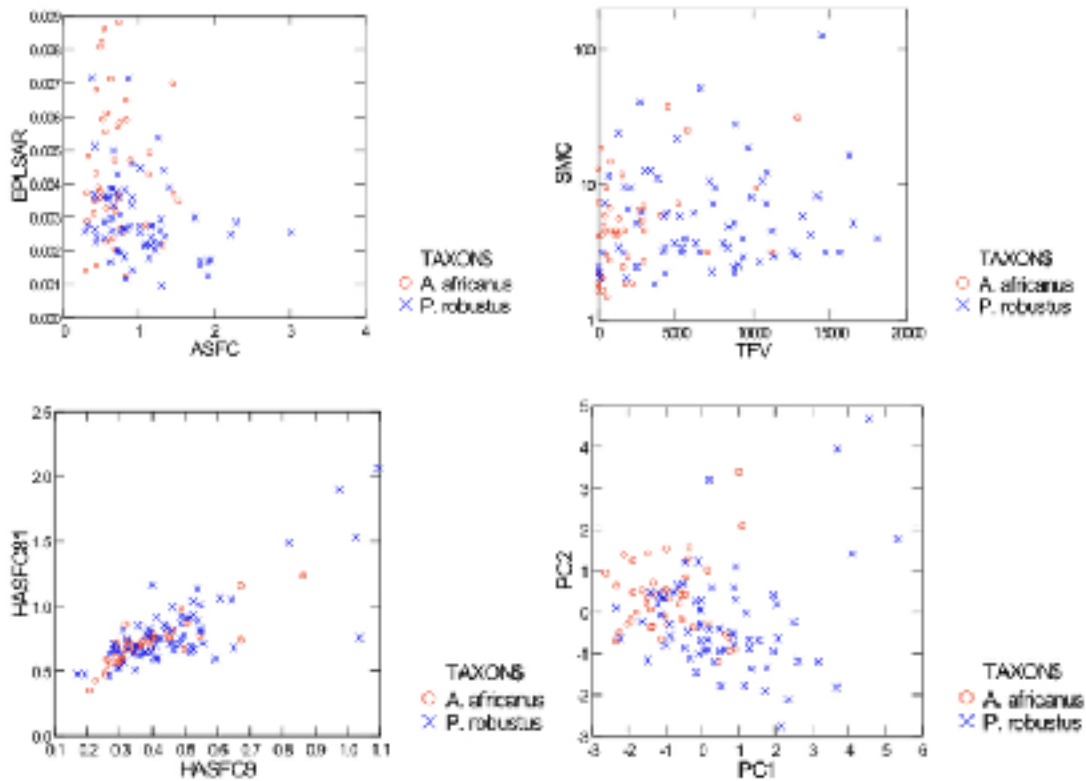
Figure 8: Bivariate plots showing comparisons of SSFA variables between taxa in central tendencies. A principle component analysis is also included comparing P. robustus and Au. africanus.

Scatter plots comparing soft filtered microwear variable differences between taxa (Fig. 8) appear to show a wider range of *epLsar* values for *Au. africanus,* ranging from .001 to .009*,* while *P. robustus* anisotropy values have a range between 0.001 and 0.007. In contrast, *P. robustus* has a wider range of complexity values. *Au. africanus* values are all under 2.0 in *Asfc* numbers. Complexity values for *P. robustus* extend past 2.0. Higher complexity values are seen in primates that exhibit some degree of hard object feeding, as the force of crushing these objects score the enamel and cause pitting (Scott et al. 2005; Altmann 2009). Higher anisotropy values

reflect textures having a particular direction, such as parallel striations (Scott et al. 2005; Scott et al. 2006). While there is significant overlap between *Au. africanus* and *P. robustus* for these two variables, *P. robustus* is more variable in its complexity and *Au. africanus* is more variable in its anisotropy. Overall, *Au. africanus* has a higher anisotropy average and *P. robustus* has higher complexity average. This larger hominin sample is reflecting the same pattern as the previous study by Scott et al. (2005) and reflects a difference in diet between the two South African taxa. These bivariate plots also show *Tfv* values for *P. robustus* have a larger range, with *Au. africanus* textural fill numbers clustering in the lower range. The larger *Tfv* values reflect more or deeper features in the 2 – 10 μm size range. However, *Smc* appears to have a comparable range for the two taxa. The scatter plot comparing both heterogeneity variables show similar clustering for both taxa, but *P. robustus* has the larger range in both instances.

ISO parameters reflect similar aspects to surface textures for both taxa, but the range of *Au. africanus* is contained within the range of *P. robustus* (Fig. 9). Height parameters Sz and Sp (maximum height and maximum peak height, respectively) reflect a linear pattern in the bivariate plot. The values for *P. robustus* extend past the range seen for *Au. africanus*, suggesting that the height parameters are can reach a larger values in the microwear textures for *P. robustus*. Comparison of volume and area ratio parameters (Vvv and Sdr, respectively), extreme peak height and the root mean square gradient (Sdq and Sxp, respectively), and feature parameters measuring pit height and mean volume (S5v and Sdv, respectively) also follow this same general pattern. However, in all these instances, there is still significant overlap of both *Au. africanus* and *P. robustus* values. *Au. africanus* falls within the range seen for *P. robustus*, but the latter demonstrates a relatively larger range.
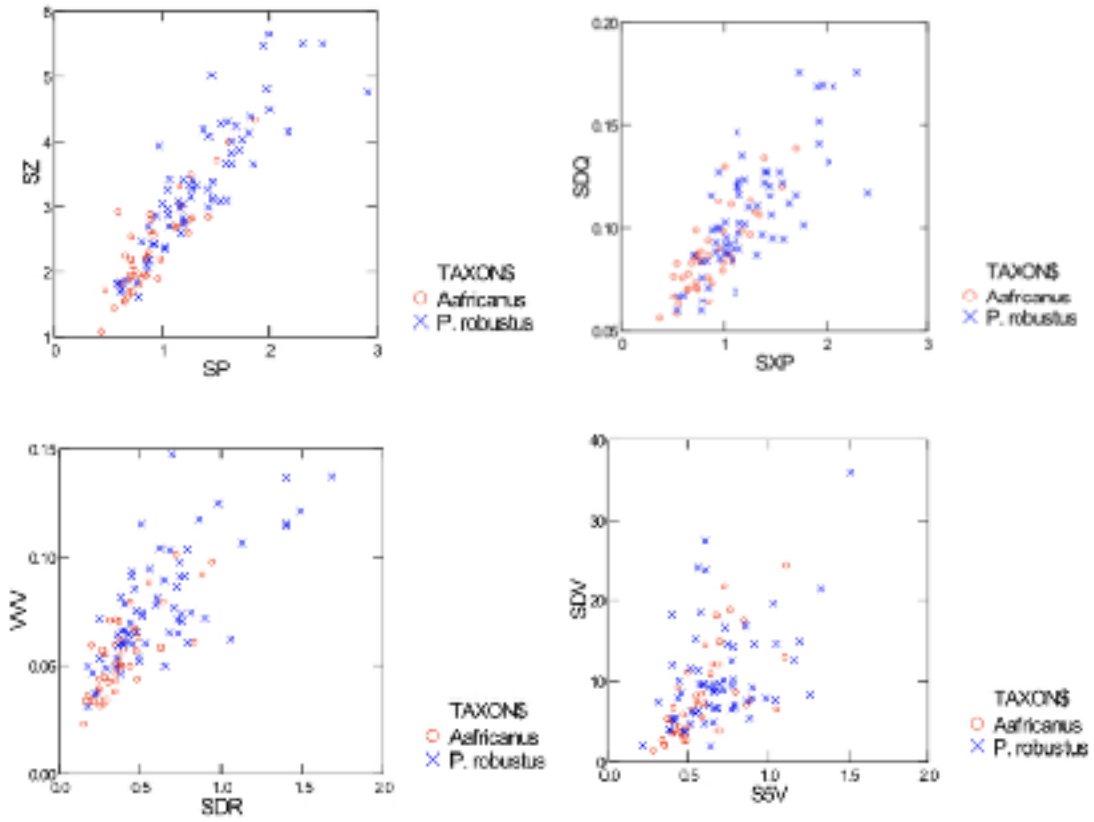
Figure 9: Bivariate plots comparing ISO parameters between taxa in central tendencies. Ssk and Sda are not included among the bivariate plots.

Table 5: MANOVA and ANOVA results comparing rank-transformed texture data for species.

Attribute	Wilk's λ	*F*-ratio	*df*	*p*-value
MANOVA	**0.525**	**5.261**	**16, 93**	**0.000**

	MS	*F*-ratio	*df*	*p*-value
Asfc	**11458.333**	**12.444**	**1, 108**	**0.001**
epLsar	**17003.788**	**19.556**	**1, 108**	**0.000**
Smc	527.424	0.516	1, 108	0.474
Tfv	**26918.523**	**34.618**	**1, 108**	**0.000**
HAsfc$_9$	**6745.606**	**6.994**	**1, 108**	**0.009**
HAsfc$_{81}$	3454.697	3.472	1, 108	0.065
Ssk	267.273	0.261	1, 108	0.611
Sp	**23520.606**	**29.069**	**1, 108**	**0.000**
Sz	**25531.856**	**32.298**	**1, 108**	**0.000**
Sxp	**22986.402**	**28.236**	**1, 108**	**0.000**
Sdq	**17309.697**	**19.973**	**1, 108**	**0.000**
Sdr	**18826.705**	**22.082**	**1, 108**	**0.000**
Vvv	**22692.273**	**27.782**	**1, 108**	**0.000**
S5v	**5970.038**	**6.144**	**1, 108**	**0.015**
Sda	3830.455	3.863	1, 108	0.052
Sdv	**7200.606**	**7.499**	**1, 108**	**0.007**

Table 6: MANOVA and ANOVA results comparing rank-transformed texture data between the sites for each species.

MANOVA	Wilk's λ	F-ratio	df	p-value
A. africanus	**0.388**	**2.667**	**16, 27**	**0.012**
P. robustus	0.278	1.077	64, 178	0.346

A. africanus

ANOVA	MS	F-ratio	df	p-value
Asfc	7.857	0.047	1, 42	0.830
epLsar	186.092	1.131	1, 42	0.294
Smc	**882.829**	**5.979**	**1, 42**	**0.019**
Tfv	113.457	0.683	1, 42	0.413
HAsfc9	156.759	0.949	1, 42	0.336
HAsfc81	105.635	0.635	1, 42	0.430
Ssk	38.029	0.226	1, 42	0.637
_Sp_	186.092	1.131	1, 42	0.294
_Sz_	121.559	0.732	1, 42	0.397
Sxp	176.035	1.069	1, 42	0.307
Sdq	64.568	0.386	1, 42	0.538
Sdr	38.029	0.226	1, 42	0.637
Vvv	53.114	0.317	1, 42	0.577
_S5v_	18.473	0.110	1, 42	0.742
Sda	**905.178**	**6.142**	**1, 42**	**0.017**
Sdv	4.225	0.025	1, 42	0.875

Table 7a-b: Levene tests for equality of variance comparing taxa, and comparing deposit grouped specimens by taxon. Swartkrans Member 3 specimen excluded from the P. robustus study because n = 1.

A. MANOVA on ranked Levene-transformed data.

	Wilks λ	F-ratio	df	p-value
Taxon comparison	0.484	6.120	16, 92	0.000
A. africanus deposits	0.340	3.272	16, 27	0.003
P. robustus deposits	0.047	3.299	64, 178	0.000

B. Post-hoc Levene tests for individual variables.

	Taxon		*A. africanus*		*P. robustus*	
	Statistic	*p*-value	Statistic	*p*-value	Statistic	*p*-value
Asfc	**7.569**	**0.007**	4.021	0.051	2.015	0.104
epLsar	**19.119**	**0.000**	2.591	0.115	2.350	0.064
Smc	1.484	0.226	**4.126**	**0.049**	**5.472**	**0.001**
Tfv	**14.136**	**0.000**	0.640	0.428	1.884	0.125
HAsfc$_9$	1.370	0.244	0.339	0.563	2.322	0.067
HAsfc$_{81}$	3.577	0.061	0.363	0.550	**6.888**	**0.000**
Ssk	0.081	0.776	0.855	0.360	1.884	0.125
Sp	**7.588**	**0.007**	1.341	0.253	**2.770**	**0.035**
Sz	**5.078**	**0.026**	1.554	0.220	2.214	0.078
Sxp	**5.187**	**0.025**	0.680	0.414	1.862	0.129
Sdq	**6.098**	**0.015**	**4.527**	**0.039**	1.656	0.172
Sdr	**9.875**	**0.002**	**5.177**	**0.028**	1.721	0.157
Vvv	**5.484**	**0.021**	1.166	0.286	1.756	0.150
S5v	1.043	0.310	0.015	0.903	1.091	0.369
Sda	0.029	0.865	3.112	0.085	0.588	0.673
Sdv	0.115	0.736	**7.230**	**0.010**	2.319	0.067

Table 8. Pairwise Levene tests of significant variables (see Table 6) for *P. robustus* deposits.

P. robustus deposits	*Smc*		*HAsfc₈₁*		*Sp*	
	Statistic	*p*-value	Statistic	*p*-value	Statistic	*p*-value
Drimolen x Kromdraai	1.256	0.281	**9.160**	**0.009**	2.880	0.112
Drimolen x Swart M1 HR	**13.775**	**0.001**	0.225	0.637	0.067	0.797
Drimolen x Swart M1 LB	0.000	0.989	**7.808**	**0.014**	2.805	0.115
Drimolen x Swart M2	1.302	0.274	0.034	0.856	1.186	0.296
Kromdraai x Swart M1 HR	0.011	0.918	**15.996**	**0.000**	**4.484**	**0.040**
Kromdraai x Swart M1 LB	**21.375**	**0.002**	0.019	0.893	0.423	0.536
Kromdraai v. Swart M2	**6.670**	**0.049**	2.256	0.193	6.380	0.053
Swart M1 HR x Swart M1 LB	**81.693**	**0.000**	**15.227**	**0.000**	**4.230**	**0.046**
Swart M1 HR v. Swart M2	1.959	0.169	0.160	0.691	2.944	0.094
Swart M1 LB x Swart M2	**22.846**	**0.003**	1.887	0.219	**7.341**	**0.035**

Australopithecus africanus vs. Paranthropus robustus

Mutivariate tests are all significant, reflecting that there are significant differences between the two South African taxa (Table 5). ANOVA tests with central tendencies show significant variation between taxa for *Asfc* (p = 0.001), *epLsar* (p = 0.000), *Tfv* (p = 0.000), and *HAsfc₉* (p = 0.009) (Table 4). *HAsfc₉* divides the surface of the scan into a 3x3 grid in order to assess how similar each of those areas are to one another (Scott et al. 2006). At this coarser scale, there are significant differences between taxa. *epLsar* values are significantly different, with *Au. africanus* exhibiting the higher anisotropy numbers when looking at the raw medians.

These results suggest that the microwear textures seen on *P. robustus* specimens have larger

features seen at coarse scales, and exhibit less directionality than *Au. africanus*.

ISO parameters were also significantly different in all but two variables (Table 5). *Ssk*

reflects the density of scratches on the surface and *Sda* measures the area of features (Delezene et

al. 2016). Neither of these variables were significantly different, showing that the amount of

scratches and the area of surface textures are not significantly different. Height parameters *Sp*

and *Sz* measure the maximum peak height and the maximum height of the surface, the latter

being the difference between the highest and lowest points of the surface (Schulz et al. 2013). In

both cases, *P. robustus* exhibits larger values that are significantly different from *Au. africanus* (p

= 0.000 for both parameters). Functional parameters *Sxp* and *Vvv* measure extreme peak height

difference and void volume, respectively (Schulz et al. 2013). Both parameters are also

significantly difference with p-values of p = 0.000 for each parameter. These parameters further

show different peak heights between taxa, as well as differences among the volume of features

(Delezene et al. 2016).

Both hybrid parameters also have significant p-values (p = 0.000). *Sdq* is the root mean

square gradient, which is calculated by taking the root mean square of all the slopes on the

surface (Blateyron 2013). *Sdr* is the developed interfacial area ratio and is a measure of

complexity (Delezene et al. 2016). Finally, feature parameters *S5v*, or the five-point pit height,

and *Sdv*, or mean dale volume. *S5v* is a measure of the depth of features, measuring the height of

pits, while *Sdv* is a volume measurement, specifically measuring the dale, or the volume of a

closed off feature (ie. a pit) (Schulz et al. 2013; Delezene et al. 2016). *S5v* is significant at p =

0.015 and the numbers are higher in *P. robustus*, indicating that the depth of features are

significantly deeper in *P. robustus*. *Sdv* is also significant at p = 0.007, and suggests that the areas are larger for *P. robustus*.

Looking at dispersion between the two taxa, there are significant differences for *Asfc* (p = 0.007) and *epLsar* (p = 0.000), as well as *Tfv* (p = 0.000). *Smc* and both heterogeneity variables are not significantly different. The Levene's tests are also significantly different for the following ISO parameters: Sp (p = 0.007), Sz (p = 0.026), Sxp (p = 0.025), Sdq (p = 0.015), Sdr (p =0.002), and Vvv (p =0.021) (Table 8). All the feature parameters were not significantly different. Additionally, Ssk (skewness) is not significantly different.

So, for complexity, anisotropy, and textural fill, there were significant differences in both central tendencies and dispersion. Additionally, all the ISO parameters that were significantly different in dispersion were also significantly different in central tendencies.

Paranthropus robustus Site Comparisons

The multivariate test results show no significant differences among central tendencies among the sites for *P. robustus* (Table 6). Interestingly, there are significant differences among *Au. africanus* sites, reporting a significant result (p = 0.012) in the MANOVA results. The ANOVA results show differences in *Smc* (p = 0.019) and *Sda* (p = 0.017) for *Au. africanus* central tendencies. However, there are some differences in dispersion for both *Au. africanus* sites as well as *P. robustus* sites. The MANOVA results are significant for sites within both taxa (Table 7a). For dispersion among *Au. africanus* sites, *Smc* (p = 0.049) is the only SSFA variable that is significantly different. Sdq (p = 0.039), Sdr (p = 0.028), and Sdv (p = 0.010) are the ISO parameters that are significantly different (Table 7b). For dispersion among *P. robustus* sites,

Smc (p = 0.001) is also significantly different. *HAsfc$_{81}$* (p = 0.000) is also significantly different, as is *Sp* (p =0.035) (Table 6b).

Because the Levene tests for equality of variance were significant for *Smc, HAsfc$_{81}$,* and *Sp*, further pairwise Levene tests were conducted between each pair of *P. robustus* bearing sites. Significant pairwise tests are highlighted in Table 7. Of note is the test between the Hanging Remnant and Lower Bank samples of Swartkrans Member 1, which were significantly different for all three variables considered. Additionally of note are the tests between Swartkrans Member 2 and Drimolen, as well as Swartkrans Member 2 and Member 1 Hanging Remnant, which are not significantly different.

Discussion

There were two principal aims of this project: 1) to expand the sample of *P. robustus* to include as many deposits as possible in order to assess whether we still see the same pattern as was reported in initial studies based on more limited samples (Grine 1986; Scott et al. 2005) and 2) to assess if there are significant differences among *P. robustus* bearing sites. Those differences can then be assessed to determine if they are consistent with feeding behaviors associated with dietary hypotheses involving fallback or suboptimal food processing.

Expanding the Paranthropus robustus sample

The original microwear texture baseline analyzed by Scott et al. (2005) demonstrated a higher proportion of anisotropic textures and lower average complexity in *Au. africanus* while there was a higher proportion of complex textures and lower average anisotropy in *P. robustus*. It was also noted that there was considerable overlap in the complexity-anisotropy bivariate space between the two species. This pattern holds true in our expanded sample. There are differences in complexity and anisotropy for each taxon, with *P. robustus* having the more complex textures and *Au. africanus* having the higher anisotropy values. Additionally, the same complexity-anisotropy overlap can also be seen in bivariate plots of the expanded samples. There is some separation of *Au. africanus* and *P. robustus*, but also a considerable amount of overlap. This suggests that while *Au. africanus* and *P. robustus* may have differing adaptations for different dietary extremes, their everyday foods are similar. This is similar to how chimpanzees and gorillas have considerable overlap in diet (Remis, 2002; Harrison and Marshall, 2011).

Overall, *Au. africanus* microwear textures reflect more tough object feeding, with higher anisotropy values and lower complexity values, while *P. robustus* reflects hard object feeding with lower anisotropy and higher complexity. Among ISO textures, *P. robustus* values were significantly larger among variables that were significantly different, reflecting features that characterize a rougher topography. This increased complexity associated with pitting and deep features with taller peaks on the surface is consistent with hard object feeding, which makes these impressions on the tooth (Scott et al. 2005; Scott et al. 2012; Calendra et al. 2013).

The significant differences for *Asfc* and *HAsfc9* evidently reflect differences in features at coarser scales. The combined *P. robustus* sample shows high average *HAsfc9* values, meaning that on a 3x3 grid, the features in each of the boxes are more heterogenous. This is also in line with the significantly different *Asfc* values, which are higher in *P. robustus* than in *Au. africanus*. This is consistent with more pitted, larger and more variability in microwear features for *P. robustus* than for *Au. africanus*. Thus, the differences between the textures of these two species becomes apparent, with *P. robustus* having a surface dominated by deep features, often pitting, creating a surface that is highly irregular, presumably from crushing hard foods, whereas *Au. africanus* likely ate foods that cause more regular, anisotropic features, such as aligned striations, in comparison to *P. robustus*. This is also supported by the significant differences in dispersion.

Paranthropus robustus bearing sites

There were no significant differences in central tendency for among *P. robustus* site samples, but there were significant differences in dispersion. This seems to imply that while the *P. robustus* food preferences are relatively consistent between the samples, there is some

variation in microwear textures, which might suggest variation in the range of foods (at least in terms of fracture properties responsible for microwear texture pattern) consumed at the times and places represented by these different deposits. It should be noted, though, that the sample sizes for the different deposits are quite different, and some of the variance seen in dispersion might be an artifact of this. This is especially so given that all the deposits are reconstructed as having a mixed woodland and grassland habitat to some degree, which will inevitably have a wide range of foods with variable material properties (Wood and Strait 2004). While there was some differences in dispersion among sites, there was no consistent pattern of difference. Interestingly, the Hanging Remnant sample and the Lower Bank sample are significantly different from one another. Both deposits are part of Member 1, with Member 2 cutting in-between the eroded space between the deposits (Brain 1981). This may suggest that there are some differences between the two deposits, though weather it is a record of changes in dietary behaviors through time is not conclusive.

Early studies of *Paranthropus* made the distinction between *Paranthropus* and *Homo*, characterizing *Paranthropus* as a stenotopic species adapted for hard object feeding, while *Homo* was considered a generalist able to exploit a wider range of habitats and foods within them (Wood and Strait 2004). This dichotomy between the stenotopic *Paranthropus* and the euryotopic *Homo* was used to explain why *Paranthropus* eventually went extinct while *Homo* flourished (Potts 1998; Constantino and Wood 2004; Wood and Strait 2004). The microwear evidence suggests that this model may be an oversimplification. In an examination of criteria associated with stenotopy and euryotopy, taking into consideration population dynamics, dietary evidence, and morphological characteristics, Wood and Strait (2004) suggested that only tooth

morphology showed a narrow specialization (a broad, flat surface for crushing harder objects). Ten other criteria suggested a more euryotopic species, implying that the genus *Paranthropus* is more generalized that originally thought (Wood and Strait 2004).

While it has been cautioned that there may be no one-to-one correspondence between dietary variability and microwear texture dispersion (Schulz et al., 2013), it is most parsimonious to suggest that the broad range of values for most microwear texture attributes seen for *P. robustus* reflects access to a food supply that was variable in its material properties. Scott et al. (2005) proposed that the variation in texture complexity seen in *P. robustus* reflects occasional hard object feeding, either as a part of the daily or seasonal diet or as a fallback resource. The larger sample continues to show those patterns. This inferred flexibility in diet further supports the idea that *P. robustus* was a euryotopic species (Wood and Strait, 2004), and consumed a wide range of foods with varying fracture properties and mechanical challenges. These differences may also be attributed to seasonal variation, but a conclusive reconstruction is not clear based solely on microwear (Gogarten and Grine 2013).

Conclusions

This project expands upon the microwear texture work done by Scott et al. (2005) on *Paranthropus robustus* and *Australopithecus africanus*. The study increases the sample size of *P. robustus* microwear textures from *n* = 9 to *n* = 66 and incorporates larger samples from Kromdraai and Swartkrans, as well as a new sample from Drimolen. The *Au. africanus* sample has been expanded to include more specimens from Sterkfontein and new material from Makapangsgat, done by E. Abella. This larger sample shows the same pattern of differences between *P. robustus* and *Au. africanus* originally identified with the smaller sample. It also expands the constellation of attributes considered for a more comprehensive characterization of microwear textures.

Paranthropus. robustus has a higher complexity average and lower anisotropy, consistent with a diet involving some degree of hard object feeding. *Australopithecus africanus* has a higher anisotropy average and lower complexity average, reflecting a diet with more tough objects. *Tfv* values are also higher in *P. robustus*, reflecting deeper features than seen in *Au. africanus*. Additionally, at a course scale, *P. robustus* exhibits more heterogenous textures than *Au. africanus*. Considering ISO parameters, only *Ssk* and *Sda* were not significantly different. The remaining parameters were all larger for *P. robustus*, indicating that features for *P. robustus* textures were had deeper pits with larger volumes, and higher peaks. These roughness parameters show more topographic relief for the textures of *P. robustus,* especially concerning pitting, and further support the conclusion that *P. robustus* was engaging in occasional hard object feeding. Additionally, the large sample size increases the variation seen in complexity textures for *P. robustus* overall.

Among *P. robustus* bearing deposits, there are no significant differences among central tendencies, but there are differences between sites when considering dispersion. There are no consistent patterns in the differences in pairwise tests between individual sites for both SSFA and ISO values. So, while these differences do suggest some degree of dietary variation among different deposits, particularly in the toughness and hardness of the objects, the variation is not overtaking the overall variation seen in the species. Currently, it is unclear as to the extent to which differences in dispersion reflect variation in environments, particularly because the current paleoenvironmental reconstructions for all South African hominin sites lack any significant differences (Wood and Strait 2004; Grine in press).

Overall, the microwear textures for *P. robustus* continue to reflect occasional hard object feeding while increasing the known variation seen in microwear textures for the species. Within species variation is also seen in dispersion, but these differences are not outside the possible range of variation seen in *P. robustus*, and central tendencies are not different among sites. While there are still unanswered questions regarding exactly what is causing the differences in dispersion among various deposits, whether it is dietary or environmental changes driving the different dispersion ranges, it does suggest that *P. robustus* is consuming a wider variety of food items with variable mechanical properties. This further lends evidence to support *P. robustus* being a more euryotopic species rather than a dietary specialist focus on hard objects (Wood and Strait 2004).

Appendix

Appendix Table 1: Complete list of P. robustus specimens used in this study.

Specimen	Species	Microwear Preserved
DNH 1	*Paranthropus robustus*	Y
DNH 3	*Paranthropus robustus*	Y
DNH 10	*Paranthropus robustus*	Y
DNH 14	*Paranthropus robustus*	N
DNH 15	*Paranthropus robustus*	Y
DNH 18	*Paranthropus robustus*	N
DNH 19	*Paranthropus robustus*	Y
DNH 21	*Paranthropus robustus*	Y
DNH 22a	*Paranthropus robustus*	Y
DNH 40	*Paranthropus robustus*	Y
DNH 46	*Paranthropus robustus*	N
DNH 47	*Paranthropus robustus*	N
DNH 51	*Paranthropus robustus*	Y
DNH 54	*Paranthropus robustus*	Y
DNH 57B	*Paranthropus robustus*	N
DNH 60	*Paranthropus robustus*	N
DNH 67	*Paranthropus robustus*	N
DNH 68	*Paranthropus robustus*	Y
DNH 74	*Paranthropus robustus*	N
DNH 75	*Paranthropus robustus*	N
KB 5063	*Paranthropus robustus*	Y
KB 5083	*Paranthropus robustus*	N
KB 5222	*Paranthropus robustus*	Y
SK 1	*Paranthropus robustus*	Y
SK5	*Paranthropus robustus*	Y

Appendix Table 1 (Cont.): Complete list of P. robustus specimens used in this study.

Specimen	Species	Microwear Preserved
SK 6	*Paranthropus robustus*	Y
SK 10/1648	*Paranthropus robustus*	Y
SK 11	*Paranthropus robustus*	Y
SK 12	*Paranthropus robustus*	N
SK 13	*Paranthropus robustus*	Y
SK 16/1591	*Paranthropus robustus*	Y
SK 17	*Paranthropus robustus*	N
SK 21	*Paranthropus robustus*	Y
SK 22/880	*Paranthropus robustus*	N
SK 23	*Paranthropus robustus*	Y
SK 25	*Paranthropus robustus*	Y
SK 31	*Paranthropus robustus*	Y
SK 34	*Paranthropus robustus*	Y
SK 36	*Paranthropus robustus*	N
SK 37	*Paranthropus robustus*	N
SK 41	*Paranthropus robustus*	N
SK 42	*Paranthropus robustus*	Y
SK 46	*Paranthropus robustus*	Y
SK47	*Paranthropus robustus*	N
SK 48	*Paranthropus robustus*	Y
SK 49	*Paranthropus robustus*	Y
SK 55	*Paranthropus robustus*	Y
SK 57	*Paranthropus robustus*	N
SK 61	*Paranthropus robustus*	Y
SK 63	*Paranthropus robustus*	Y
SK 74	*Paranthropus robustus*	Y

Appendix Table 1 (Cont.): Complete list of P. robustus specimens used in this study.

Specimen	Species	Microwear Preserved
SK 75	*Paranthropus robustus*	N
SK79	*Paranthropus robustus*	N
SK 81	*Paranthropus robustus*	N
SK 83	*Paranthropus robustus*	N
SK 89	*Paranthropus robustus*	Y
SK 98	*Paranthropus robustus*	N
SK 102	*Paranthropus robustus*	N
SK 104	*Paranthropus robustus*	N
SK 105	*Paranthropus robustus*	Y
SK 826	*Paranthropus robustus*	Y
SK 826A/877	*Paranthropus robustus*	N
SK 826B	*Paranthropus robustus*	N
SK 829	*Paranthropus robustus*	N
SK 831A	*Paranthropus robustus*	Y
SK 832	*Paranthropus robustus*	Y
SK 834	*Paranthropus robustus*	Y
SK 835	*Paranthropus robustus*	N
SK 836	*Paranthropus robustus*	N
SK 837	*Paranthropus robustus*	Y
SK 838	*Paranthropus robustus*	Y
SK 839	*Paranthropus robustus*	N
SK 840	*Paranthropus robustus*	N
SK 841B	*Paranthropus robustus*	Y
SK 844	*Paranthropus robustus*	Y
SK 846A	*Paranthropus robustus*	Y
SK 849	*Paranthropus robustus*	N

Appendix Table 1 (Cont.): Complete list of P. robustus specimens used in this study.

Specimen	Species	Microwear Preserved
SK 851	*Paranthropus robustus*	N
SK 855	*Paranthropus robustus*	N
SK 858	*Paranthropus robustus*	N
SK 862	*Paranthropus robustus*	Y
SK 870	*Paranthropus robustus*	Y
SK 871	*Paranthropus robustus*	N
SK 872	*Paranthropus robustus*	N
SK 876	*Paranthropus robustus*	Y
SK 877	*Paranthropus robustus*	N
SK 1587	*Paranthropus robustus*	N
SK 1588	*Paranthropus robustus*	Y
SK 1590	*Paranthropus robustus*	N
SK 3974	*Paranthropus robustus*	Y
SK 3975	*Paranthropus robustus*	N
SK 3976	*Paranthropus robustus*	N
SK 3977	*Paranthropus robustus*	N
SK 10642/10643	*Paranthropus robustus*	N
SK 10645	*Paranthropus robustus*	N
SK 14000	*Paranthropus robustus*	Y
SK 14003	*Paranthropus robustus*	Y
SK 14133	*Paranthropus robustus*	N
SKW 5	*Paranthropus robustus*	N
SKW 8	*Paranthropus robustus*	N
SKW 10	*Paranthropus robustus*	N
SKW 11	*Paranthropus robustus*	Y
SKW 14	*Paranthropus robustus*	Y

Appendix Table 1 (Cont.): Complete list of P. robustus specimens used in this study.

Specimen	Species	Microwear Preserved
SKW 29	*Paranthropus robustus*	N
SKW 3114	*Paranthropus robustus*	N
SKW 4767	*Paranthropus robustus*	N
SKW 4769	*Paranthropus robustus*	N
SKX 334	*Paranthropus robustus*	Y
SKX 3355	*Paranthropus robustus*	Y
SKX 3601	*Paranthropus robustus*	Y
SKX 4446	*Paranthropus robustus*	Y
SKX 5002	*Paranthropus robustus*	Y
SKX 5013	*Paranthropus robustus*	N
SKX 5014	*Paranthropus robustus*	Y
SKX 5023	*Paranthropus robustus*	Y
SKX 19892	*Paranthropus robustus*	Y
SKX 21841	*Paranthropus robustus*	N
TM 1517	*Paranthropus robustus*	Y
TM 1536	*Paranthropus robustus*	N
TM 1600	*Paranthropus robustus*	Y
TM 1603	*Paranthropus robustus*	N

Bibliography

Adams JW, Rovinsky DS, Herries AIR, Menter CG. 2016. Macromammalian faunas, biochronology and palaeoecology of the early Pleistocene Main Quarry hominin-bearing deposits of the Drimolen Palaeocave System, South Africa. PeerJ 4:e1941; DOI 10.7717/peerj.1941.

Altmann SA. 2009. Fallback Foods, Eclectic Omnivores, and the Packaging Problem. American Journal of Physical Anthropology 140:615-629.

Arman SD, Ungar PS, Brown CA, DeSantis LRG, Schmidt C, Prideaux GJ. 2015. Minimizing inter-microscope variability in dental microwear texture analysis. Surface Topography: Metrology and Properties 4:1-22.

Avery DM. 1995. A Preliminary Assessment of the Micromammalian Remains from Gladysvale Cave, South Africa. Palaeont. Afr. 32:1-10.

Avery DM. 2001. The Plio-Pleistocene vegetation and climate of Sterkfontein and Swartkrans, South Africa, based on micromammals. Journal of Human Evolution 41:113-132.

Backwell LR and d'Errico F. 2001. Evidence of termite foraging by Swartkrans early hominids. Proceedings of the National Academy of Sciences 98:1358-1363.

Backwell L and d'Errico F. 2008. Early hominid bone tools from Drimolen, South Africa. Journal of Archaeological Science 35:2880-2894.

Baker G, Jones LHP, Wardrop ID. 1959. Cause of wear in sheep teeth. Nature 184:1583-1584.

Blateyron F. 2013. The Areal Field Paramters. In: Leach R, editor. Characterisation of Areal Surface Texture. Berlin:Springer. p 15-43.

Bock WJ and von Wahlert G. 1965. Adaptation and the Form-Function Complex. Evolution 19:269-299.

Brain CK. 1981. The Hunters or the Hunted? An Introduction to African Cave Taphonomy. Chicago: University of Chicago Press.

Brain CK. 1993a. The Occurrence of Burnt Bones at Swartkrans and Their Implications for the Control of Fire by Early Hominids. Transvaal Museum Monographs 8:229-249.

Brain CK. 1993b. Structure and Stratigraphy of the Swartkrans Cave in the Light of New Excavations. Transvaal Museum Monographs 8:23-33.

Brain CK and Shipman P. 1993. The Swartkrans Bone Tools. In: Swartkrans: A Cave's Chronicle of Early Man. p 195-215.

Broom R. 1938. The Pleistocene Anthropoid Apes of South Africa. Nature 142:377-379.

Broom R and Robinson JT. 1952. Paranthropus crassidens type. Transvaal Museum Memoirs 6:1-3.

Brown CA and Siegmann S. 2001. Fundamental scales of adhesion and area-scale fractal analysis. International Journal of Machine Tools and Manufacture 41:1927-1933.

Butler PM. 1952. The milk molars of Perissodactyla, with remarks on molar occlusion. Proceedings of the Zoological Society of London 121:777-817.

Calandra I, Schulz E, Pinnow M, Krohn S, Kaiser ™. 2012. Teasing apart the contributions of hard dietary items on 3D dental microtextures in primates. Journal of Human Evolution 63:85-98.

Carrion JS and Scott L. 1999. The challenge of pollen analysis in palaeoenvironmental studies of hominid beds: the record from Sterkfontein caves. Journal of Human Evolution 36:401-408.

Cerling TE, Mbua E, Kirera FM, Manthi FK, Grine FE, Leakey MG, Sponheimer M, Uno KT. 2011. Diet of Paranthropus boisei in the early Pleistocene of Africa. Proceedings of the National Academy of Sciences 108:9337-9341.

Cofran Z, Thackeray JF. 2010. One or two species? A morphometric comparison between Robust Australopithecines from Kromdraai and Swartkrans. South African Journal of Science 106:40-44.

Conover WI and Iman RL. 1981. Rank transformations as a bridge between parametric and nonparametric statistics. The American Statistician 35:124-129.

Constantino PJ, Lee JJW, Chai H, Zipfel B, Ziscovici C, Lawn BR, Lucas PW. 2010. Tooth chipping can reveal the diet and bite forces of fossil hominins. Biol. Lett. 6:826-829.

Constantino PJ, Lucas PW, Lee JJW, Lawn BR. 2009. The Influence of Fallback Foods on Great Ape Tooth Enamel. American Journal of Physical Anthropology 140:653-660.

Constantino P and Wood B. 2004. Paranthropus paleobiology. In: Miscela´nea en homenaje a Emiliano Aguirre, Volumen III. Paleoantropologia. Madrid: Museo Arqueolo´cico Regional. p 136–151.

Constantino PJ and Wright BW. 2009. The Importance of Fallback Foods in Primate Ecology and Evolution. American Journal of Physical Anthropology 140:599-602.

Daegling DJ, Judex S, Ozcivici E, Ravosa MJ, Taylor AB, Grine FE, Teaford MF, Ungar PS. 2013. Viewpoints: Feeding Mechanics, Diet, and Dietary Adaptations in Early Hominins. American Journal of Physical Anthropology 151:356-371.

Daegling DJ and McGraw WS. 2007. Functional Morphology of the Mangabey Mandibular Corpus: Relationship to Dental Specializations and Feeding Behavior. American Journal of Physical Anthropology 134:50-62.

Daegling DJ, McGraw WS, Ungar PS, Pampush JD, Vick AE, Bitty A. 2011. Hard-Object Feeding in Sooty Mangabeys (Cercocebus atys) and Interpretation of Early Hominin Feeding Ecology. PLoS ONE 6:e23095. doi:10.1371/journal.pone.0023095.

Delezene LK, Teaford MF, Ungar PS. 2016. Canine and Incisor Microwear in Pitheciids and Ateles Reflects Documented Patterns of Tooth Use. American Journal of Physical Anthropology 161:6-25.

de Ruiter DJ. 2003. Revised faunal lists for Members 1-3 of Swartkrans, South Africa. Annals of the Transvaal Museum 40:29-41.

de Ruiter DJ. 2004. Undescribed hominin fossils from the Transvaal Museum faunal collectioons. Annals of the Transvaal Museum 41:29-40.

de Ruiter DJ, Sponheimer M, Lee-Thorp JA. 2008. Indications of habitat association of Australopithecus robustus in the Bloubank Valley, South Africa. Journal of Human Evolution 55:1015-1030.

Gibbon RJ, Pickering TR, Sutton MB, Heaton JL, Kuman K, Clarke RJ, Brain CK, Granger DE. 2014. Cosmogenic nuclide burial dating of hominin-bearing Pleistocene cave deposits at Swartkrans, South Africa. Quaternary Geochronology 24:10-15.

Gogarten JF and Grine FE. 2013. Seasonal Mortality Patterns in Primates: Implications for the Interpretation of Dental Microwear. Evolutionary Anthropology 22:9-19.

Grine FE. 1981. Trophic Differences Between "Gracile" and "Robust" Australopithecines: A Scanning Electron Microscope Analysis of Occlusal Events. South African Journal of Science 77:203-230.

Grine FE. 1986. Dental Evidence for Dietary Differences in Australopithecus and Paranthropus: a Quantitative Analysis of Permanent Molar Microwear. Journal of Human Evolution 15:783-822.

Grine FE. 1989. New Hominid Fossils From the Swartkrans Formation (1979-1986 Excavations): Craniodental Specimens. American Journal of Physical Anthropology 79:409-449.

Grine, FE. 1993. Description and preliminary analysis of new hominid craniodental fossils from the Swartkrans Formation. In: Brain CK, editor. Swartkrans: A Cave's Chronicle of Early Man. Transvaal Museum, Pretoria. p 75-116.

Grine FE and Daegling DJ. 1993. New mandible of Paranthropus robustus from Member 1, Swartkrans Formation, South Africa. Journal of Human Evolution 24:319-333.

Grine FE, Sponheimer M, Ungar PS, Lee-Thorp J, Teaford MF. 2012. Dental Microwear and Stable Isotopes Inform the Paleoecology of Extinct Hominins. American Journal of Physical Anthropology 148:285-317.

Grine FE and Strait DS. 1994. New hominid fossils from Member 1 "Hanging Remnant", Swartkrans Formation, South Africa. Journal of Human Evolution 26:57-75.

Grine FE, Ungar PS, Teaford MF. 2002. Error Rates in Dental Microwear Quantification Using Scanning Electron Microscopy. Scanning 24:144-153.

Grine FE, Ungar PS, Teaford MF. 2006. Was the Early Pliocene hominin 'Australopithecus" anamensis a hard object feeder?. South African Journal of Science 102:301-310.

Grine FE, Ungar PS, Teaford MF, El-Zaatari S. 2013. Molar Microwear, Diet and Adaptation in a Purported Hominin Species Lineage from the Pliocene of East Africa. In: Reed KE, Fleagle JG, Leakey RE, editors. The Paleobiology of Australopithecus. Springer. p 213-223.

Harrison ME and Marshall AJ. 2011. Strategies for the Use of Fallback Foods in Apes. International Journal of Primatology 32:531-565.

Herries AIR, Curnoe D, Adams JW. 2009. A multi-disciplinary seriation of early Homo and Paranthropus bearing paleocaves in southern Africa. Quaternary International 202:14-28.

Hylander WL. 1975. Incisor size and diet in anthropoids with special reference to Cercopithecidae. Science 189:1095-1098.

Johanson DC and White TD. 1979. A Systematic Assessment of Early African Hominids. Science 203:321-330.

Jolly CJ. 1970. The seed-eaters: a new model of hominid differentiation based on a baboon

analogy. Man 5:5-26.

Kay RF. 1977. The Evolution of Molar Occlusion in the Cercopithecidae and Early Catarrhines. American Journal of Physical Anthropology 46:327-352.

Kay RF. 1985. Dental Evidence for the Diet of Australopithecus. Ann. Rev. Anthropol. 14:315-341.

Keyser AW. 2000. The Drimolen Skull: the most complete australopithecine cranium and mandible to date. South African Journal of Science 96:189-193.

Keyser AW, Menter CG, Moggi-Cecchi J, Pickering TR, Berger LR. 2000. Drimolen: a new hominid-bearing site in Gauteng, South Africa. South African Journal of Science 96:193-197.

Kimbel WH, White TD, Johanson DC. 1998. Implications of KNM-WT 17000 for the Evolution of "Robust" Australopithecus. In: Grine FE, editor. Evolutionary History of the 'Robust' Australopithecines. New York: A. de Gruyter. p 259-268.

King T, Andrews P, Boz B. 1999. Effect of Taphonomic Precesses on Dental Microwear. American Journal of Physical Anthropology 108:359-373.

Kruger KL, Scott JR, Kay RF, Ungar PS. 2008. Technical Note: Dental Microwear Textures of "Phase I" and "Phase II" Facets. American Journal of Physical Anthropology 137:485-490.

Lambert JE. 2009. Summary to the Symposium Issue: Primate Fallback Strategies as Adaptive Phenotypic Plasticity—Scale, Pattern, and Process. American Journal of Physical Anthropology 140:759-766.
Lambert JE, Chapman CA, Wrangham RW, Conklin-Brittain NL. 2004. Hardness of Cercopithecine Foods: Implications for the Critical Function of Enamel Thickness in Exploiting Fallback Foods. American Journal of Physical Anthropology 125:363-368.

Lee-Thorp JA, Sponheimer M, Luyt J. 2007. Tracking changing environments using stable carbon isotopes in fossil tooth enamel: an example from the South African hominin sites. Journal of Human Evolution 53:595-601.

Lee-Thorp J, Thackeray JF, van der Merwe N. 2000. The hunters and the hunted revisited. Journal of Human Evolution 39:565-576.

Lucas P, Constantino P, Wood B, Lawn B. 2008. Dental enamel as a dietary indicator in mammals. BioEssays 30:374-385.

Lucas PW, Corlett RT, Luke DA. 1984. Plio-Pleistocene Hominid Diets: an Approach Combining Masticatory and Ecological Analysis. Journal of Human Evolution 14:187-202.

McKee JK, Thackeray JF, Berger LR. 1995. Faunal Assemblage Seriation of Southern African Pliocene and Pleistocene Fossil Deposits. American Journal of Physical Anthropology 96:235-250.

Mills JRE. 1955. Ideal dental occlusion in primates. Dental Practice 6:47-51.

Moggi-Cecchi J, Menter C, Boccone S, Keyser A. 2010. Early hominin dental remains from the Plio-Pleistocene site of Drimolen, South Africa. Journal of Human Evolution 58:374-405.

Olejniczak AJ, Smith TM, Skinner MM, Grine FE, Feeney RNM, Thackeray JF, Hublin JJ. 2008. Three-dimensional molar enamel distribution and thickness in Australopithecus and Paranthropus. Biol. Lett. 4:406-410.

Partridge TC. 1985. The paleoclimatic significance of Cainozoic terrestrial stratigraphic and tectonic evidence from southern Afria: a review. South African Journal of Scient 81:245-247.

Perneger TV. 1998. What's wrong with Bonferroni adjustments. Brit Med J 316(7139): 1236–1238.

Potts R. 1998. Environmental Hypotheses of Hominin Evolution. Yearbook of Physical Anthropology 41:93-136.

Purnell MA, Crumption N, Gill PG, Jones G, Tayfield EJ. 2013. Within-guild dietary discrimination from 3-D textural analysis of tooth microwear in insectivorous mammals. Journal of Zoology 291:249-257.

Rak Y. 1983. The Australopithecine Face. New York: Academic Press.

Remis MJ. 2002. Food Preferences Among Captive Western Gorillas (Gorilla gorilla gorilla) and Chimpanzees (Pan troglodytes). International Journal of Primatology 23:231-249.

Robinson JT. 1954a. The Genera and Species of the Australopithecinae. American Journal of Physical Anthropology 12:181-200.

Robinson JT. 1954b. Prehominid Dentition and Hominid Evolution. Evolution 8:324-334.

Rose JC and Ungar PS. 1998. Gross Dental Wear and Dental Microwear in Historical Perspective. In: Alt KW, Rosing FW, Teschler-Nicola M, editors. Dental Anthropology: Fundamentals, Limits and Prospects. New York: Springer.

Rovinsky DS, Herries AIR, Menter CG, Adams JW. 2015. First description of in situ primate and faunal remains from the Plio-Pleistocene Drimolen Makondo palaeocave infill, Gauteng, South Africa. Palaeontologica Electronica 18:1-21.

Ryan AS and Johanson DC. 1989. Anterior dental microwear in Australopithecus afarensis: comparisons with human and nonhuman primates. Journal of Human Evolution 18:235-268.

Schulz E, Piotrowski V, Clauss M, Mau M, Merceron G Kaiser ™. 2012. Dietary Abrasiveness is Associated with Variability of Microwear and Dental Surface Texture in Rabbits. PLoS ONE 8:e56167. doi:10.1371/journal.pone.0056167.

Scott RS, Teaford MF, Ungar PS. 2012. Dental Microwear Textures and Anthropoid Diets. American Journal of Physical Anthropology 147:551-579.

Scott RS, Ungar PS, Bergstrom TS, Brown CA, Grine FE, Teaford MF, Walker A. 2005. Dental microwear textures analysis shows within-species diet variability in fossil hominins. Nature 436:693-695.

Scott RS, Ungar PS, Bergstrom TS, Brown CA, Childs BE, Teaford MF, Walker A. 2006. Dental microwear texture analysis: technical considerations. Journal of Human Evolution 51:339-349.

Simpson GG. 1933. Paleobiology of Jurassic mammals. Paleobiologica 5:127-158.

Skelton RR and McHenry HM. 1998. Trait list bias and a reappraisal of early hominid phylogeny. Journal of Human Evolution 34:109-113.

Smith AL, Benazzi S, Ledogar JA, Tamvada K, Pryor Smith LC, Weber GW, Spencer MA, Lucas PW, Michael S, Shekeban A, Al-Fadhalah K, Almusallam AS, Dechow PC, Grosse IR, Ross CF, Madden RH, Richmond BG, Writ BW, Wang Q, Byron C, Slice DE, Wood S, Dzialo C, Berthaume MA, Van Casteren A, Strait DS. 2014. The Feeding Biomechanics and Dietary Ecology of Paranthropus boisei. The Anatomical Record 298:145-167.

Sponheimer M, Lee-Thorp J, de Ruiter D, Codron D, Codron J, Baugh AT, Thackeray F. 2005. Hominins, sedges, and termites: new carbon isotope data from the Sterkfontein valley and Kruger National Park. Journal of Human Evolution 48:301-312.

Sponheimer M, Passey BH, de Ruiter DJ, Guatelli-Steinberg D, Cerling TE, Lee-Thorp JA. 2006. Isotopic Evidence for Dietary Variability in the Early Hominin Paranthropus robustus. Science 314:980-982.

Strait DS, Constantino P, Lucas PW, Richmond BG, Spencer MA, Dechow PC, Ross CF, Grosse IR, Wright BW, Wood BA, Weber GW, Wang Q, Byron C, Slice DE, Chalk J, Smith AL, Smith LC, Wood S, Berthaume M, Benazzi S, Dzialo C, Tamvada K, Ledogar JA. 2013. Viewpoints: Diet and Dietary Adaptations in Early Hominins: The Hard Food Perspective. American Journal of Physical Anthropology 151:339-355.

Strait DS, Grine FE, Moniz MA. 1997. A reappraisal of early hominid phylogeny. Journal of Human Evolution 32:17-82.

Strait DS, Grosse IR, Dechow PC, Smith AL, Wang Q, Weber GW, Neubauer S, Slice DE, Chalk J, Richmond BG, Lucas PW, Spencer MA, Schrein C, Wright BW, Byron C, Ross CF. 2010. The Structural Rigidity of the Cranium of Australopithecus africanus: Implications for Diet, Dietary Adaptations, and the Allometry of Feeding Biomechanics. The Anatomical Record 293:583-593.

Strait DS, Richmond BG, Spencer MA, Ross CF, Dechow PC, Wood BA. 2007. Masticatory biomechanics and its relevance to early hominid phylogeny: an examination of palatal thickness using finite-element analysis. Journal of Human Evolution 52:585-599.

Strait DS, Weber GW, Constantino P, Lucas PW, Richmond BG, Spencer MA, Dechow PC, Ross CF, Grosse IR, Wright BW, Wood BA, Want Q, Byron C, Slice DE. 2012. Microwear, mechanics and the feeding adaptations of Australopithecus africanus. Journal of Human Evolution 62:165-168.

Strait DS, Weber GW, Neubauer S, Chalk J, Richmond BG, Lucas PW, Spencer MA, Schrein C, Dechow PC, Ross CF, Grosse IR, Wright BW, Constantino P, Wood BA, Lawn B, Hylander WL, Wang Q, Byron C, Slice DE, Smith AL. 2008. The feeding biomechanics and dietary ecology of Australopithecus africanus. Proc. Natl. Acad. Sci. 106:2124-2129.

Strait DS and Wood BA. 1999. Early hominid biogeography. Proc. Natl. Acad. Sci. 96:9196-9200.

Strait SG. 1993. Molar Morphology and Food Textures Among Small-Bodied Insectivorous Mammals. J. Mamm. 74:391-402.

Suwa G, Asfaw B, Beyene Y, White TD, Katoh S, Nagaoka S, Nakaya H, Uzawa K, Renne P, WoldeGabriel G. 1997. The first skull of Australopithecus boisei. Nature 389:489-492.

Teaford MF. 1988. A review of dental microwear and diet in modern mammals. Scanning Microscopy 2:1149-1166.

Thackeray JF, de Ruiter DJ, Berger LR, van der Merwe NJ. 2001. Hominid fossils from Kromdraai: a revised list of specimens discovered since 1938. Annals of the Transvaal

Museum 38:43-56.

Thackeray JF, Kirschvink JL, Raub TD. 2002. Palaeomagnetic analyses of calcified deposits from the Plio-Pleistocene hominid site of Kromdraai, South Africa. South African Journal of Science 98:537-540.

Ungar PS. 1995. A Semiautomated Image Analysis Procedure for the Quantification of Dental Microwear II. Scanning 7:57-59.

Ungar PS. 2007c. Dental topography and human evolution with comments on the diets of Australopithecus africanus and Paranthropus. In: Bailey SE and Hublin JJ, editors. Dental Perspectives on Human Evolution. Springer. p 321-343.

Ungar PS, Brown CA, Bergstrom TS, Walker A. 2003. Quantification of Dental Microwear by Tandem Scanning Confocal Microscopy and Scale-Sensitive Fractal Analyses. Scanning 25:185-193.

Ungar PS and Grine FE. 1991. Incisor size and wear in Australopithecus africanus and Paranthropus robustus. Journal of Human Evolution 20:313-340.

Ungar PS, Grine FE, Teaford MF. 2008. Dental Microwear and Diet of the Plio-Pleistocene Hominin Paranthropus boisei. PLoS ONE e2044. doi:10.1371/journal.pone.0002044.

Ungar PS and Hlusko LJ. 2016. The evolutionary path of least resistance. Science 353:29-30.

Ungar PS, Scott RS, Grine FE, Teaford MF. 2010. Molar microwear textures and the diets of Australopithecus anamensis and Australopithecus afarensis. Phil. Trans. R. Soc. B 365:3345-3354.

Ungar PS, Simon JC, Cooper JW. 1991. A Semiautomated Image Analysis Procedure for the Quantification of Dental Microwear. Scanning 13:31-36.

Ungar PS and Sponheimer M. 2011. The Diets of Early Hominins. Science 334:190-193.

Vrba ES. 1981. The Kromdraaai Australopithecine Site Revisited in 1980; Recent Investigations and Results. Annals of the Transvaal Museum 33:17-60.

Walker A. 1981. Dietary Hypotheses and Human Evolution. Philosophical Transactions of the Royal Society of London 292:57-64.

Walker A, Leakey RE, Harris JM, Brown FH. 1986. 2.5-myr Australopithecus boisei from west of Lake Turkana, Kenya. Nature 322:517-522.

Walker A and Teaford M. 1989. Inferences from Quantitative Analysis of Dental Microwear.

Wood B and Constantino P. 2007. Paranthropus boisei: Fifty Years of Evidence and Analysis. Yearbook of Physical Anthropology 50:106-132.

Wood B and Strait D. 2004. Patterns of resource use in early Homo and Paranthropus. Journal of Human Evolution 46:119-162.

Wright BW, Wright KA, Chalk J, Verderane MP, Fragaszy D, Visalberghi E, Izar P, Ottoni EB, Constantino P, Vinyard C. 2009. Fallback Foraging as a Way of Life: Using Dietary Toughness to Compare the Fallback Signal Among Capuchins and Implications For Interpreting Morphological Variation. American Journal of Physical Anthropology 140:687-699.